



Stability Analysis of 'L-Shaped' PSC Box Girder Bridge

Author

Mr. S. B. Dhobale¹, Prof. K. S. Upase²

¹Student, M.E. Structures, Department of Civil Engineering, M.S. Bidve Engg College, Latur-413512

Email: *siddheshwar.dhobale@yahoo.com*

²Associate Professor, M.E. Structures, Department of Civil Engineering, M.S. Bidve Engg. College, Latur -413512

Email: *ksu_upase@yahoo.co.in*

ABSTRACT

The structural behaviour of box girder is complicated, which is difficult to analyse in its actual conditions by conventional methods. Prestress technology has been a part of the 'Bridge Design Practice Manual' since the 1960 edition. Over the years, revisions and updates have been made. Again, there is a need for updating. This edition reflects revised friction coefficients and detailed computer output.

In present study a two lane, two cell box girder bridge made up of prestressed concrete is analysed for moving loads as per IRC:6 recommendations, Prestressed Code (IS: 1343) and also as per IRC: 18 specifications. The analysis of PSC box girder using 'SAP 2000-12 Bridge wizard'. The various span/depth ratios considered to get the proportioning depth at which stresses criteria and deflection criteria get satisfied. The contribution of prestressing steel is incorporated, while the material and geometric nonlinear analysis of plane prestressed concrete frames including the time dependent effects due to load & temperature history, creep, shrinkage, and aging of concrete and relaxation of prestress were also considered. For the construction stage analysis, many sophisticated computer programs for the analysis of segmentally erected prestressed concrete bridges considering the time-dependent effects of concrete has been developed to predict the bridge response.

Prestressing tendons may be stressed, prestressed, and removed, while a traveling formwork can be modelled. However, most computer programs have some limitations in wide use because of complexities in practical applications.

Keywords: *Concrete Box Girder Bridge, Prestress Force, Eccentricity, Prestress Losses, Reinforcement, Tendons, Flexure strength, shear strength, Analysis and computation. SAP Model.*

INTRODUCTION

Bridge construction today has achieved a worldwide level of importance. Bridges are the key elements in any road network. Use of box girder is gaining popularity in bridge engineering fraternity because of its better stability, serviceability, economy, aesthetic appearance and structural efficiency. The structural behavior of box girder is complicated, which is difficult to analyze in its actual conditions by conventional methods.

Prestress concrete is ideally suited for the construction of medium and long span bridges. Ever since the development of prestressed concrete by Freyssinet in the early 1930s, the material has found extensive application in the construction of long-span bridges, gradually replacing steel which needs costly maintenance due to the inherent disadvantage of corrosion under aggressive environment conditions. One of the most commonly used forms of superstructure in concrete bridges is precast girders with cast-in-

situ slab. This type of superstructure is generally used for spans between 20 to 40 m.

Prestress technology has been a part of the Bridge Design Practice Manual since the 1960 edition. Over the years, revisions and updates have been made. Again, there is a need for updating. This edition reflects revised friction coefficients and detailed computer output.

In present study a two lane simply supported Box Girder Bridge made up of prestressed concrete which is analysis for moving loads as per Indian Road Congress (IRC:6) recommendations, Prestressed Code (IS: 1343) and also as per IRC: 18 specifications. The analyzed of box girder using SAP 2000 14 Bridge Wizard and prestressed with parabolic tendons in which utilize full section. The various span/ depth ratio considered to get the proportioning depth at which stresses criteria and deflection criteria get satisfied.

T or I-girder bridges are the most common example under this category and are very popular because of their simple geometry, low fabrication cost, easy erection or casting and smaller dead loads. In this paper study the India Road Loading considered for design of bridges, also factor which are important to decide the preliminary sizes of concrete box girders. Also considered the IRC:18-2000 for "Prestressed Concrete Road Bridges" and "Code of Practice for Prestressed Concrete " Indian Standard. Analyze the Concrete Box Girder Road Bridges for various spans, various depth and check the proportioning depth. Several research works dealing with numerical procedures based on the finite-element method for the nonlinear analysis of prestressed concrete structures were proposed during the past decades (Kang et al. 1977, 1980; Scordelis 1983, 1984, 1988). The contribution of prestressing steel is incorporated, while the material and geometric nonlinear analysis of plane prestressed concrete frames including the time dependent effects due to load history, temperature history, creep, shrinkage, and aging of concrete and relaxation of prestress were also considered. For the construction stage analysis, many sophisticated computer programs

for the analysis of segmentally erected prestressed concrete bridges considering the time-dependent effects of concrete has been developed to predict the bridge response (Ketchum 1986; Cruz et al. 1991, 1994, 1998; Mari et al. 1984, 2000, 2003; Bishara et al. 1990). Changes in structural configuration and the structural effects of the load and temperature histories, materials nonlinear behavior, creep, shrinkage, aging of concrete and relaxation of prestressing steel were taken into account. Prestressing tendons may be stressed, prestressed, and removed, while a traveling formwork can be modeled. However, most computer programs have some limitations in wide use because of complexities in practical applications.

The purpose of this paper is to develop a general step-by-step procedure for the three-dimensional finite-element analysis of segmentally constructed prestressed concrete bridges. The hexahedral element, including the enhanced assumed strain technique, is employed to improve the element performances. Structural effects caused by realistic tendon profiles, load history, changes of the bridge geometry, and support movement are taken in account, while long-term effects such as creep, shrinkage, and aging of the concrete, as well as relaxation of the prestressing steel, are also incorporated. Finally, several numerical examples are presented to demonstrate the capabilities of the proposed procedure

TIME DEPENDANT EFFECTS ON PSC BOX GIRDER BRIDGE

The service behaviours of pre-stressed concrete bridges are significantly affected due to time dependent effects like, Creep, Shrinkage and ambient Temperature. These are complex phenomena and are mainly influenced by characteristics of concrete, its exposure condition, humidity of air and stages of construction, which are sequential for pre-stressed concrete structures. These time dependent effects induce additional internal forces and causes deflection to the bridge superstructure which reduces the serviceability,

durability & stability of the bridge in long run. From several studies, it is observed that due to Creep, Shrinkage and daily atmospheric temperature variation in structural concrete there is a long-term deflection in Pre-stressed concrete girders. These causes decrease in service life of bridge and in long run it required strengthening with external pre-stressing to secure its original load bearing capacity.

Creep and Shrinkage have a considerable impact upon the performance of concrete structures, causing increased deflections as well as affecting stress distribution. The variation of creep and shrinkage properties in concrete is effected by various factors commonly classified as internal and external factors, from Bazant (1985). The change of environmental conditions, such as humidity & temperature may be considered as an external factor. The variation in quality and mix composition of the materials used in the concrete may be considered as internal factors. The effects of creep, shrinkage and atmospheric temperature variations in the structures like long span bridge girders may leads to excessive deformation and widespread cracks. They also affect the sizing and setting of expansion joints due to axial shortening arising from creep and shrinkage effects along with existence of prestressing force. Both creep & shrinkage may occur concurrently and reduce the pre-stressing forces in PSC bridge girders. Thus the time dependent effects may create havoc in the serviceability, durability and stability of bridge structure. The time-dependent effects of concrete structures due to creep & shrinkage of concrete have not yet been controlled rationally despite great advances in theories & in design software. This fact results from the complexity of time dependent effects of concrete structures. Study on the various individual time effects due to creep and shrinkage in concrete structures can be found in the work of Gilbert (1988). The study conducted by Robertson (2005) in actual bridges for time dependent deflection shows that the difference between the calculated prediction and actual deflection in the bridge is

large. This difference is due to inaccurate evaluation of pre-stressing force and thermal stress due to atmospheric temperature. From the report of Zollman CC (1985) & Massicotte B (1994), it is found that when prestress losses have become excessive, additional prestressing force has to be applied to the bridge during the service stage at a great cost to maintain the serviceability. Studies of Saiidi M (1996) (1998) on the time dependent prestress loss in actual post-tensioned concrete bridges shows that the difference between the calculated prediction and the actual prestress force is large. Therefore purpose of this study is to present the type of strain development and deflection caused in PSC bridge superstructures due to time dependent effects.

2.1 Creep:

Creep phenomenon may be defined as the property of concrete by which it continues to deform with time under sustained loads at unit stresses within the acceptable elastic range (i.e. below $0.5 f'c$). It is obtained by subtracting from the total measured strain in a loaded specimen, the sum of the initial instantaneous (in elastic range) strain due to the sustained stress, the shrinkage, and the eventual thermal strain in an identical load-free specimen which is subjected to the same history of relative humidity and temperature conditions. Conveniently creep may be designated at constant stress under condition of steady relative humidity and temperature, assuming strain at loading as the instantaneous strain at anytime. The definition of creep lumps together the basic creep and the drying creep.

- a) Basic creep occurs under condition of no moisture movement to or from the environment.
- b) Drying creep occurs as an additional creep due to drying.

2.2 Shrinkage:

Shrinkage is the property of concrete to change in volume independent of the load it sustains. It is essentially due to evaporation of water from concrete and hydration of its components with

time, which occurs without any external stress to the concrete. Shrinkage is usually expressed as a dimensionless strain under steady condition of relative humidity and temperature. There are mainly three phenomena causing total shrinkage of concrete: drying shrinkage, autogenous shrinkage and carbonation shrinkage.

- a) Drying shrinkage is due to loss of moisture in the concrete.
- b) Auto genous shrinkage is due to hydration of cement.
- c) Carbonation shrinkage is due to carbonation of various cement hydration product in presence of CO₂.

2.3 Thermal Stress:

Generally concrete bridge structures are subjected to thermal effects due to the interaction with air temperature and solar radiation, leads to seasonal and daily temperature changes in the structure. The seasonal variation corresponds to the maximum mean temperature change expected to occur during the year. Due to the poor thermal conductivity of concrete, the temperature also changes hourly from the surface to the interior points of the structure and causes daily nonlinear temperature distribution across the section. As a result thermal stress will always be present within the section along the depth of the girder section. These stress variation causes development of strain variation and also deflection in the bridge girder section. Solution of the heat flow equation for different ambient conditions supported by the experimental results obtained by Emanuel and Lewis (1981) and defined critical design temperature gradients. In the past decades extensive studies have been conducted regarding temperature effects on concrete bridges (1981) (2009) (1978). The nonlinear temperature distribution that arises in concrete structures in the early days, after concreting, lead to tensile stress which may also causes cracking of young concrete.

2.4 Uncertainty Modelling of Shrinkage & Creep of concrete:

Over the years, parameters that influence creep and shrinkage of concrete were established, even though these phenomena cannot be separated from each other. These parameters allow for predicting the creep and shrinkage phenomenon and therefore the behaviour of a structure. The parameters included the water cement ratio, the curing method, the ambient humidity, the aggregates, air content and the age at loading. Several material models for shrinkage and creep of concrete have been proposed both in literature and in design codes. The commonly used models in the codes are those suggested by the ACI Committee 209R-92 (1992) and the CEB-FIP MC (1990). These two model codes are based on extensive research as well as experimental studies. In 1992 the American Concrete Institute (ACI) recommends the procedure for the prediction of creep, shrinkage and temperature effects in concrete structure in its ACI-209R-92 codal provisions. It presents the designer with a unified and designated approach to the problem of volume change in concrete. This procedure is applicable for normal weight and all the light weight concrete, using both moist and steam curing and Type I and III cement under the standard conditions as shown in Table-1. Correction factors are used for the conditions other than the standards. In 1990, the Comite Europeen du Beton (CEB) adopted new guidelines for prediction of creep and shrinkage for structural concretes, having 28 days mean cylindrical compressive strength varying from 12 to 80 Mpa, mean relative humidity 40-100% and mean temperature 5-30°C.

2.5 Comparison of predicted values from Model Codes for Shrinkage Strain & Creep compliance & collected field data's:

Arolli Bridge over Thane Creek in Navi Mumbai, India is 1030 meter long with 2 carriageways of 3lanes in each direction. It consists of 42 PSC single cell box girders of 50 meter length (c/c of pier).The width of deck slab is 14.98 meter for

each carriageway. Each main span girder is made up of precast pre-stressed single cell box girder as shown in fig- 1 with inclined web of constant 3.2 meter depth. Each box girder is supported on 4 PTFE bearings fixed on pedestals over the pier caps. The values of creep coefficient and shrinkage strain based on the prediction models

ACI 209R-92 and CEB-FIP 90 for the box girder, with respect to time is calculated by developing a computer program. The shrinkage strain and creep compliance values as obtained are plotted against age of concrete as shown in Fig- 2 & 3 respectively. Similar values are also obtained using Bridge designing software ‘Midas Civil’ for creep coefficient and shrinkage strain.

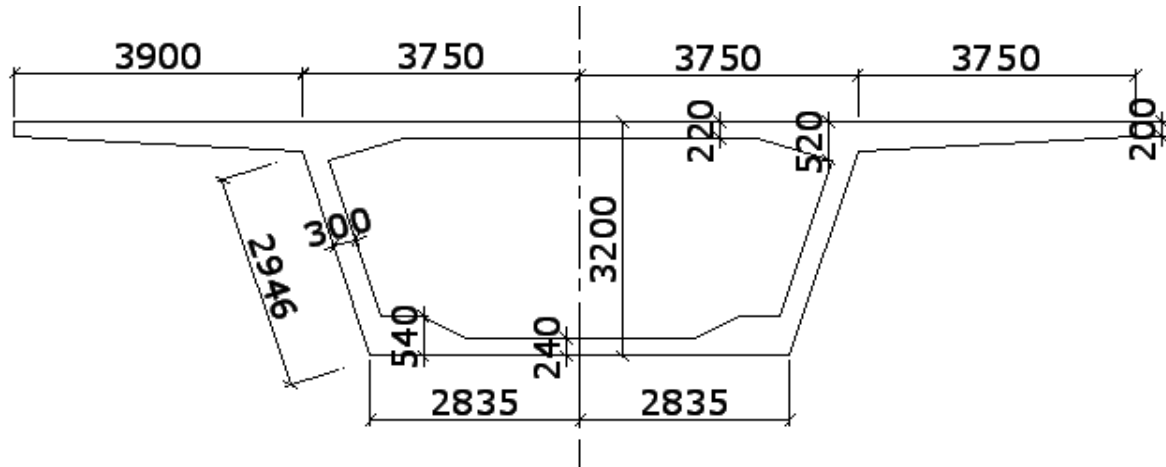


Fig.- 1. Cross section of single cell precast pre-stressed box girder

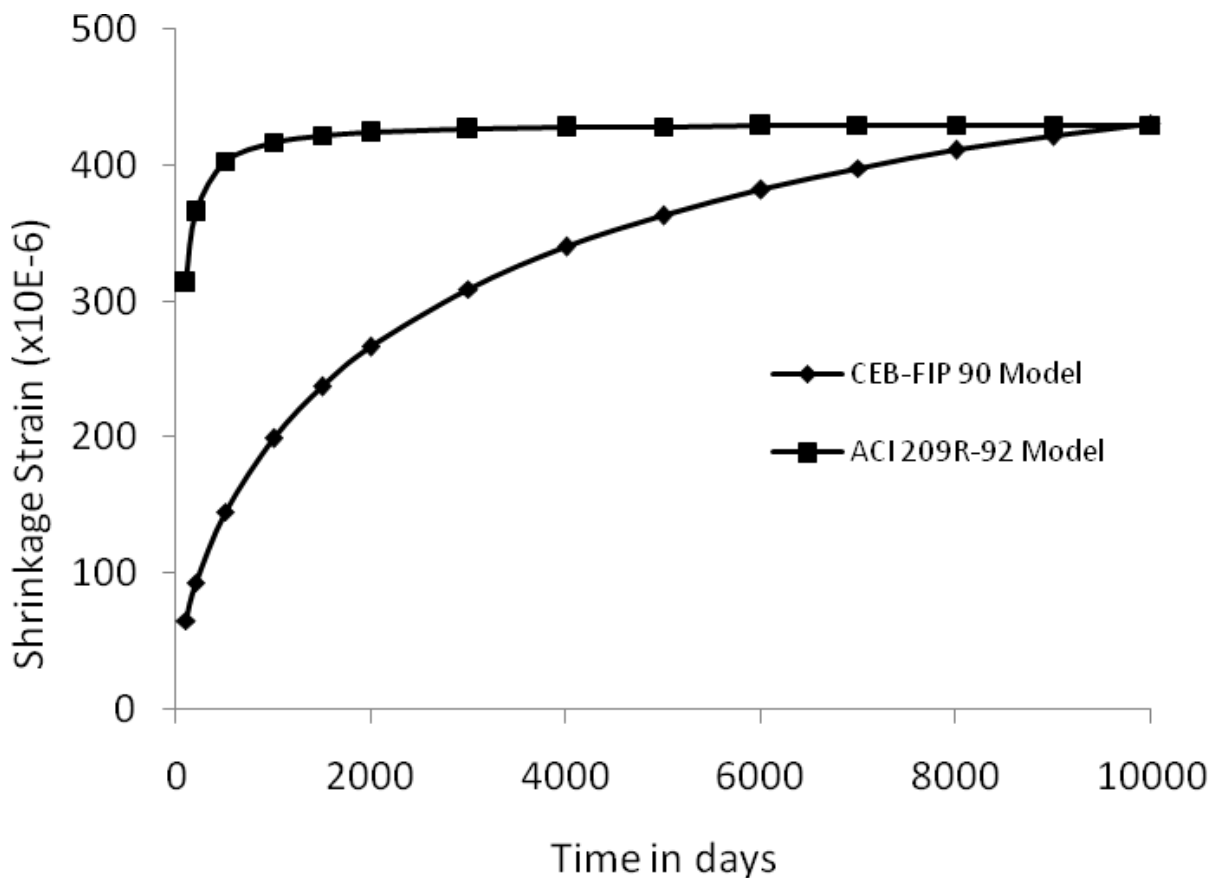


Fig.2. Prediction of Shrinkage strain using Model Codes

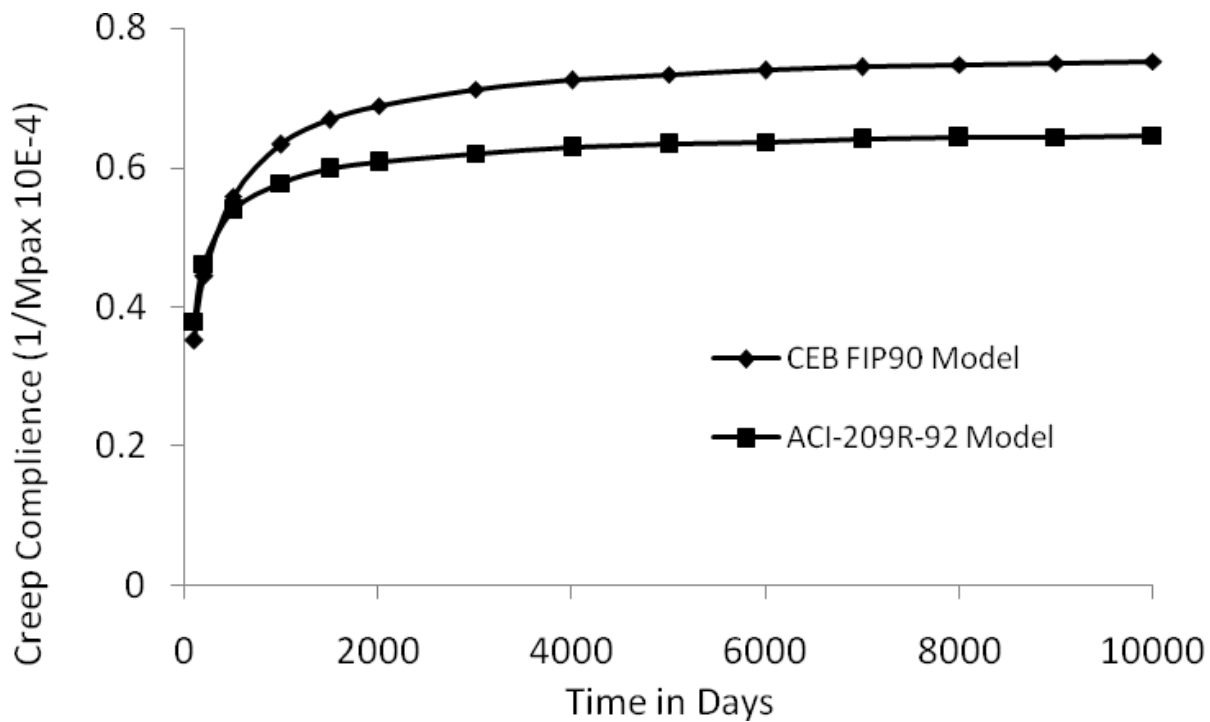


Fig. 3. Prediction of Creep Compliance using Model codes

From the fig- 2 it is observed that predicted values for shrinkage strain using ACI 209R-92 model code are larger than that using CEB-FIP 90 model code, at early age of concrete but at latter age of concrete the shrinkage strain from both the model codes are almost equal. From fig- 3 it is observed that predicted values for creep compliance using ACI 209R-92 model code are smaller than that using CEB-FIP 90 model code, at early age of concrete, but with the age of concrete the difference between the values increases. As per ACI 209R-92, the increase in creep after, say 100 to 200 days of concreting is usually more pronounced than shrinkage. The shrinkage usually increases more rapidly in percent of ultimate value, during first few weeks of concreting. The similar prediction was also observed in the work of In-Hwan Yang, (2003) for probabilistic analysis of creep and shrinkage effects in PSC box

girder bridges. Vibrating Wire strain gauges having sensitivity of $\pm 1 \mu$ were embedded at particular locations in soffit, web and deck slab of the PSC Box girder (fig-1) during concreting for collection of strain data's from field. The development of strain was monitored and recorded for approximately 800 days from the day of concreting of box girder section. A graph as shown in fig-4 is plotted based on recorded field data's for development of strain in soffit, web and deck slab of box girder with the age of concrete. From the graph (fig-4) it can be observed, that the maximum strain due to combine effect of creep and shrinkage in soffit, web and deck slabs were in and around 350 days from the day of concreting of girder. After development of maximum strain, the strain value decreases with time and become more or less constant with age of concrete.

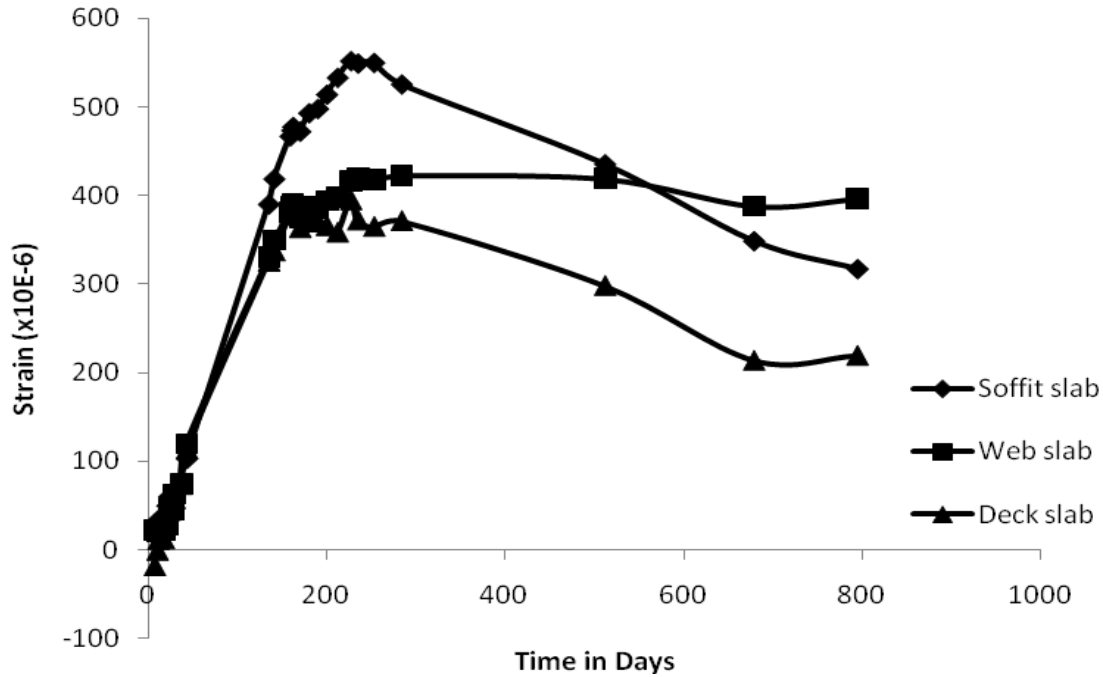


Fig.4. Development of strain with time in concrete box girder section.

On comparison between predicted values (fig-2 & 3) and real field values (fig-4) it is observed that predicted values for shrinkage strain and creep compliance are maximum at age of concrete around 350 day and there after rate of increases of strain is very nominal with time. Whereas field values shows development of maximum strains in and around 350 days from the day of concreting and thereafter strain reduces before becoming almost constant. From the graphs it can also be observed that predicted values for shrinkage strain and creep compliance as per Model Code does not show any sign of decrease with age of concrete after attaining maximum values.

2.6 Deflection of Simply Supported PSC box girder due to development of creep & shrinkage strain:

Creep and shrinkage causes continuous change in the stresses in concrete and steel in any reinforced or pre-stressed concrete members. The knowledge of this change in stress is of interest for a number of reasons. For instance, in pre-stressed concrete, we can determine the loss of pre-stress, and the time dependent deformations such as axial shortening and deflection, knowing the change in stress and the associate strains. The deflection of the Arolli Bridge girder, G-7 along the span was

recorded after application of final stage of pre-stressing and upto 390 days from the date of concreting. The effect of creep & shrinkage strain in development of deflection of girder with age of concrete is obtained on analyzing the recorded data. From the deflection pattern as shown in fig-5 it is observed that there is maximum deflection of 5.6 mm of hogging in nature, at mid span of the girder after 390 days of concreting. The deflection was measured using precession level upto accuracy of 0.1 mm in no traffic load condition. For the same single cell PSC concrete box girder the development of maximum strain (fig-4) due to creep and shrinkage of concrete was observed in and around 350 days from the day of concreting. So the effect of shortening of concrete girder due to creep and shrinkage causes the deflection at mid span and due to presence of pre-stressing force throughout the girder length the deflection caused is hogging in nature. Generally, bridge is subjected to the effects of weather changes both daily and seasonal. The phenomenon of development of temperature gradient, strain and deflection on account of such changes in ambient condition is complex. This thermal effect should be considered in the design process for serviceability limit state conditions, namely those

associated with cracking of the structure or excessive displacements.

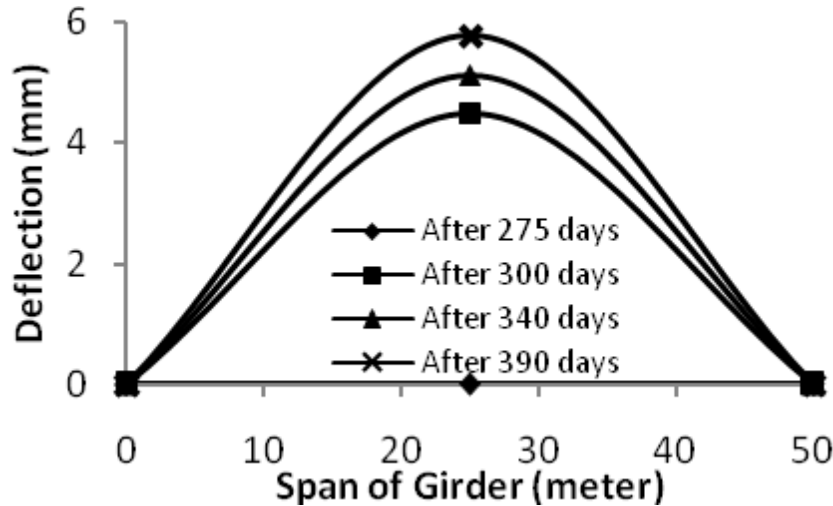


Fig. 5. Deflection profile of pre-stressed concrete Box Girder.

2.7 Effects of ambient temperature on PSC box girders:

Temperature is the major environmental factors which also influence the effect of creep and shrinkage. The effect of change in temperature on concrete creep and shrinkage is basically two-fold. First, they directly influence the time ratio rate. Second, they also affect the rate of aging of the concrete, i.e the change of material properties due to progress of cement hydration. The nonlinear temperature distribution T , in the cross section of bridge superstructures can be sub divided in a

uniform temperature T_m , in a linear gradient for each direction associated with a temperature difference T and in a nonlinear distribution T_o as shown in fig.6. The two components T_m and T are associated with the longitudinal displacements and curvatures of the bridge girder. The movement of the structures associated with these two components, can be determined by linear elastic method for statically determinate structures. For statically indeterminate structures as movements are restrained, thermal forces arise, which are required to be considered in design.



Fig. 6. Thermal stress components

2.8 Deflection and development of strain in Simply Supported PSC Box Girder due to atmospheric temperature:

The development of strain and deflections over the bridge girder, G-13 of Arolli Bridge were recorded throughout the day at different

temperature in no traffic load condition to determine the effect of atmospheric temperature. The deflection pattern of this 50 meter length girder after 600 days of concreting is obtained on analyzing the recorded data. The cross section of the PSC box girder is shown in fig-1. Deflection

measurements were carried out using high precision N3 level with an accuracy of 0.1mm. The deflection pattern of the box girder as obtained at different temperature of a day is shown in fig-7 & fig-8. Due to poor thermal conductivity of concrete, the temperature changes hourly from surface to the interior points of the bridge and

daily nonlinear temperature distribution arises. Due to this temperature variation across the section and presence of pre-stressing force along the length of the girder there is development of deflection with increase in temperature which is hogging in nature.

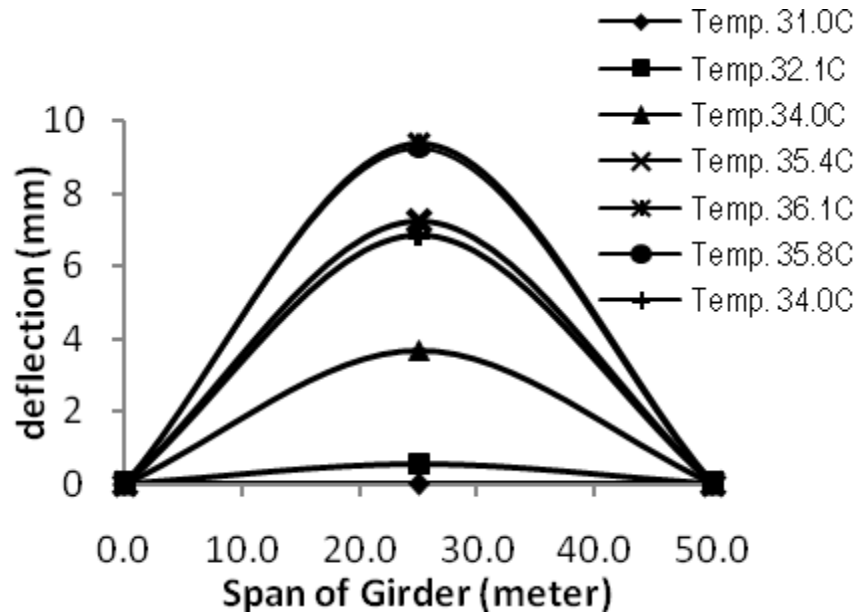


Fig.7. Pattern of deflection of box girder G-13 at different temperature

The development of strains and temperatures were obtained, using vibrating wire strain gauges embedded at mid span of the girder on soffit and deck slab. Strain development due to temperature in soffit slab and deck slab of the box girder are shown in fig-9 & fig-10 respectively. From the plotted graph it can be clearly observed that, on account of temperature rise there is development of compression in soffit slab and tension in deck slab. Due to occurrence of this different nature of strain, in soffit (compression) & deck (tension) slab there is tendency of hogging effect in the prestressed concrete box girder. The deflection

pattern is shown in fig-7 for the PSC simply supported box girder G-13. Plotting graph between temperature vs deflection as in fig-8, it is observed that with increase in 5°C (31°C to 36°C) ambient temperature during day time, there is increase in deflection of girder by 9.5mm at mid span. The deflection of PSC Girder again reduces or comes back to its original position on decrease of atmospheric temperature during night time. Daily repetition of same deflection pattern in PSC bridge girder may give rise to the formation of cracks and causes deterioration at latter age.

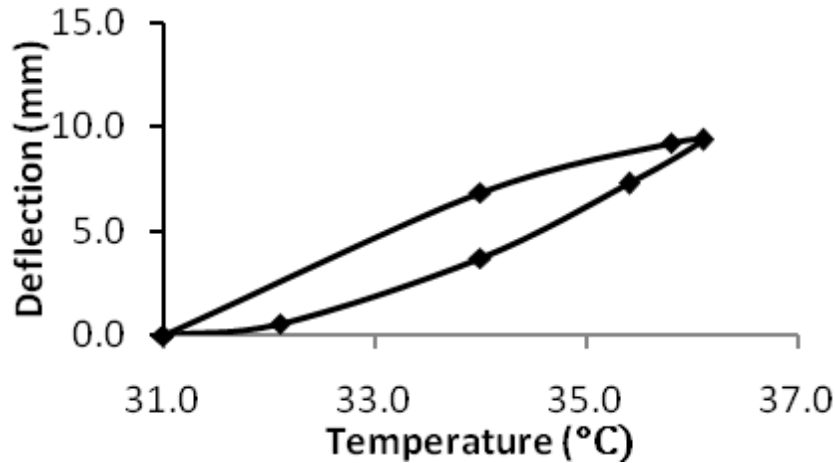


Fig.8. Temperature vs Deflection of box girder G-13

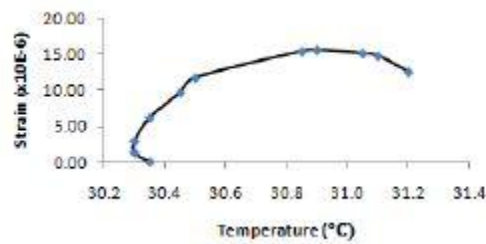


Fig. 9. Strain vs Temperature in Soffit slab of Box Girder bridge at mid span

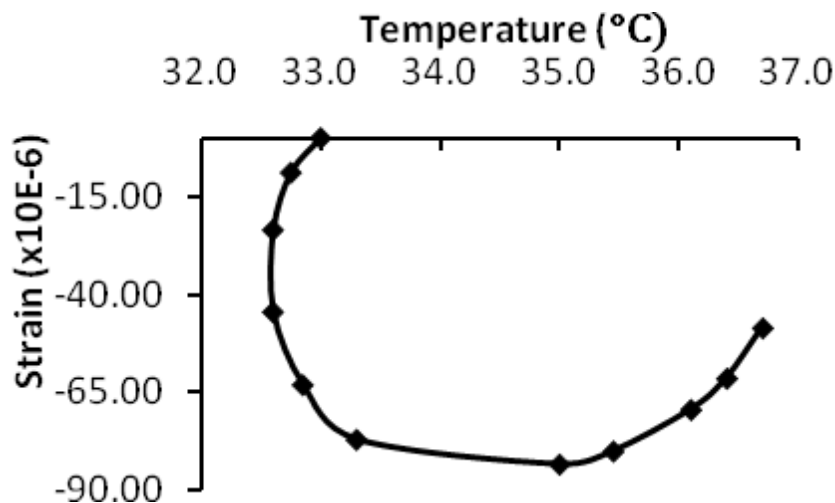


Fig.10. Strain vs Temperature in Deck slab of Box Girder Bridge at mid span

2.9 Deflection of balanced cantilever PSC box girder due to atmospheric temperature:

The Zuaribridge at Goa, India is a balanced cantilever box girder bridge with its two arms spanning on both side of the abutment. The depth of box girder varies from 8.0 m. at the pier to 2.25 m. at the tip of the cantilever arms. The length of one cantilever arm is 58.40 m. and another is 58.66 m. which are connected to the next

cantilever arm through hinges. The bridge is a single cell non-prismatic box girder having a two lane carriageway and footpath on either side. Fig-11 shows the general arrangement of the cantilever bridge girder over pier P-4. This typical case study was taken up to access the behaviour of PSC balanced cantilever box girder bridge after 15 year of service. The behaviour of the bridge in terms of deflection during day time at different

atmospheric temperature was recorded in no traffic load condition. High precision N3 level with an accuracy of 0.1mm directly, was used for

deflection measurements. The deflection of cantilever arms at different atmospheric temperature is plotted in fig.-12.

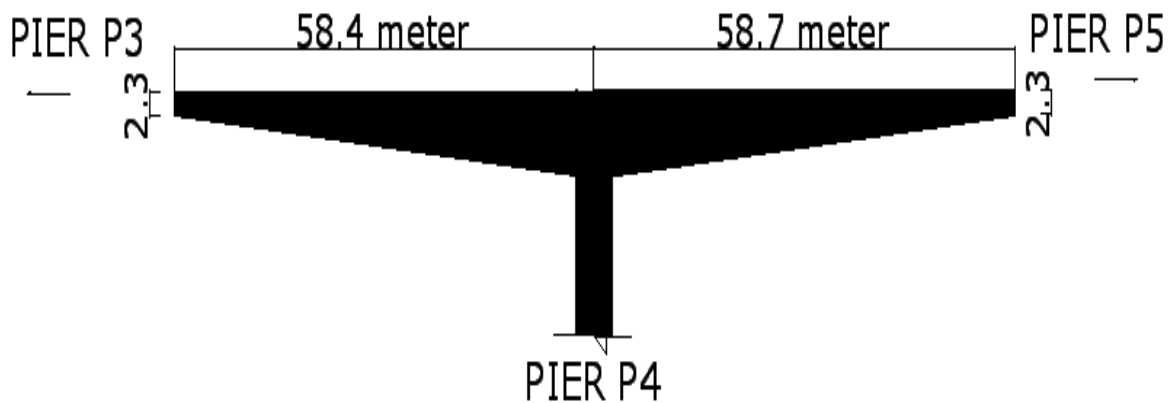


Fig.11. Elevation of pre-stressed balanced cantilever box girder P-4

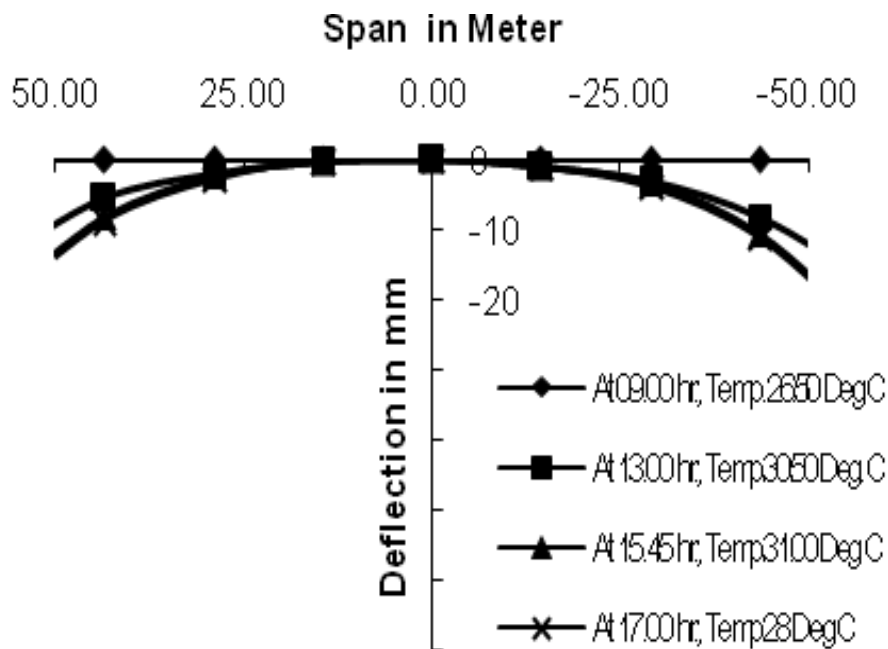


Fig.12. Deflection profile of balanced cantilever PSC bridge Girder.

From the graph it is observed that the tip of cantilevers shows downward deflection of average 24.5mm at maximum ambient temperature 31.0 °C. Plotting graph between temperature vs. deflection as shown in fig-13, it is observed that, with rise in temperature of only 4.5 °C, (26.5°C to 31.0°C) during day time there is increase in downward deflection of 24.5 mm at the tip of PSC

cantilever arms. During night hours when ambient temperature reduces, the deflection also reduces and PSC cantilever arms returns to its original position. The serviceability of the bridge has been reduced only after 15 year of construction and required to be strengthened with external pre-stressing.

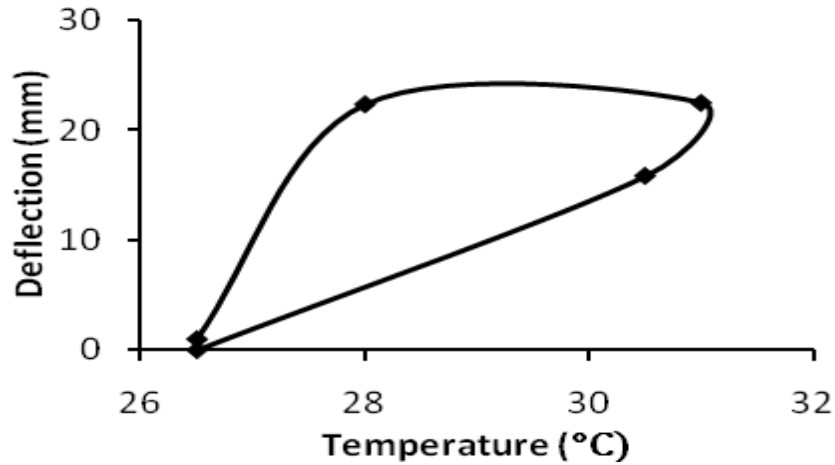
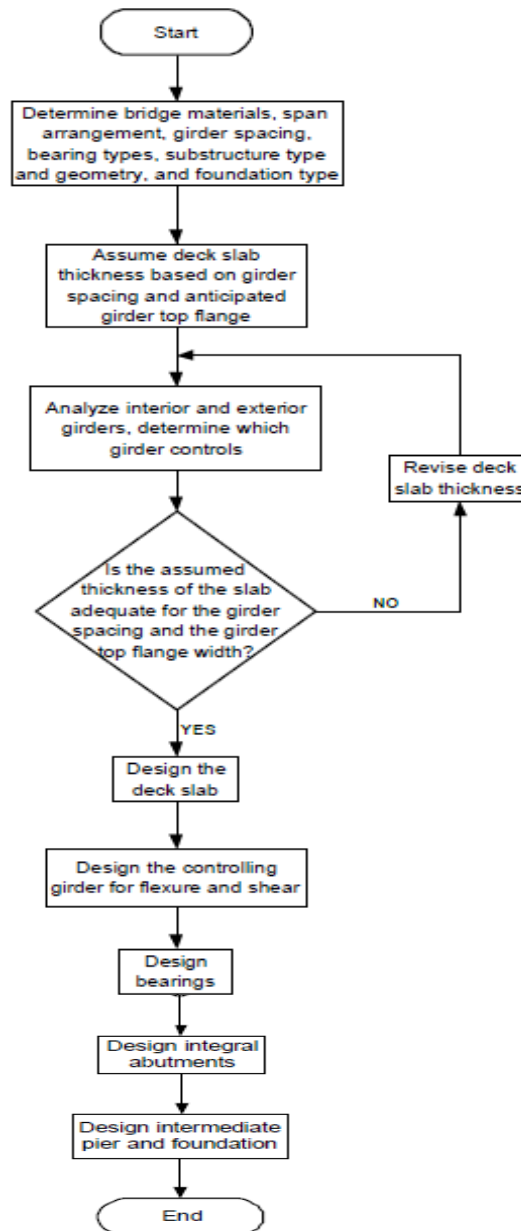


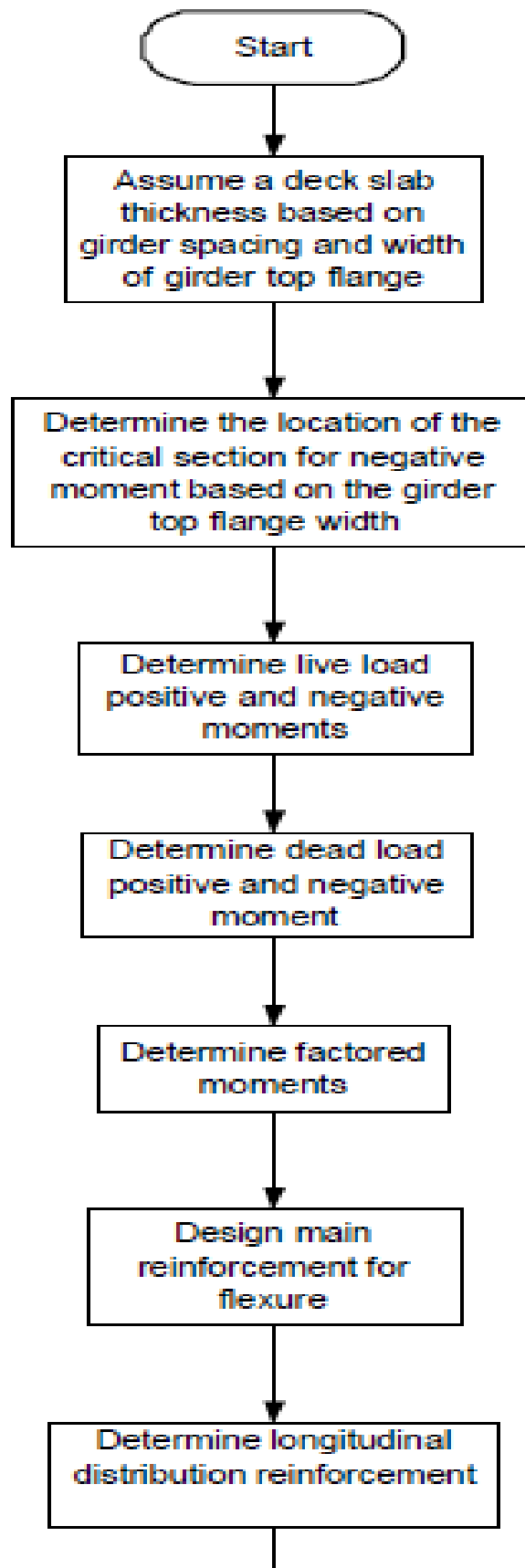
Fig.13. Temp. vs Deflection of PSC cantilever Girder

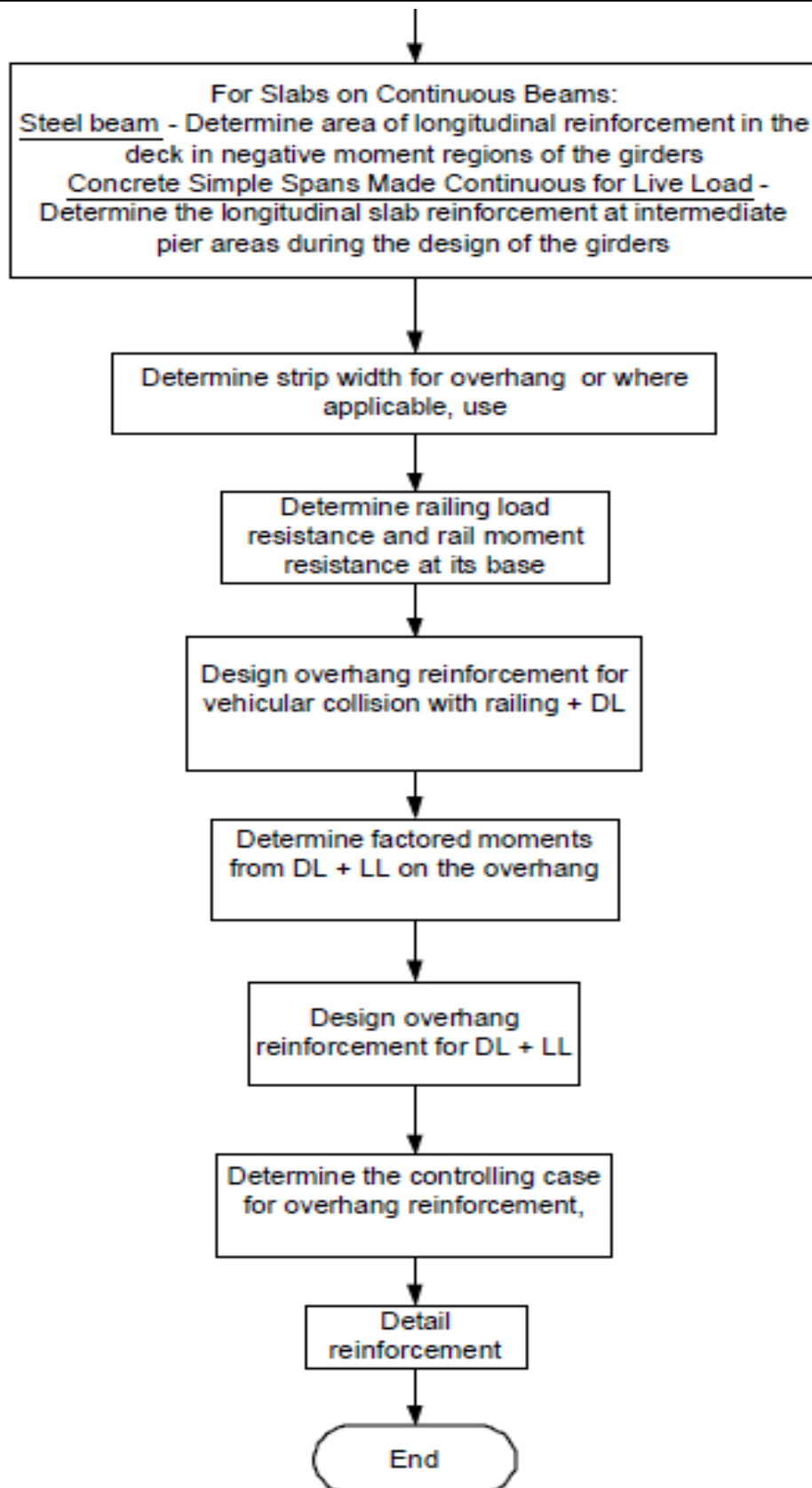
3. FLOWCHART FOR DESIGN OF PSC BOX GIRDER BRIDGE

3.1 Main Design Steps

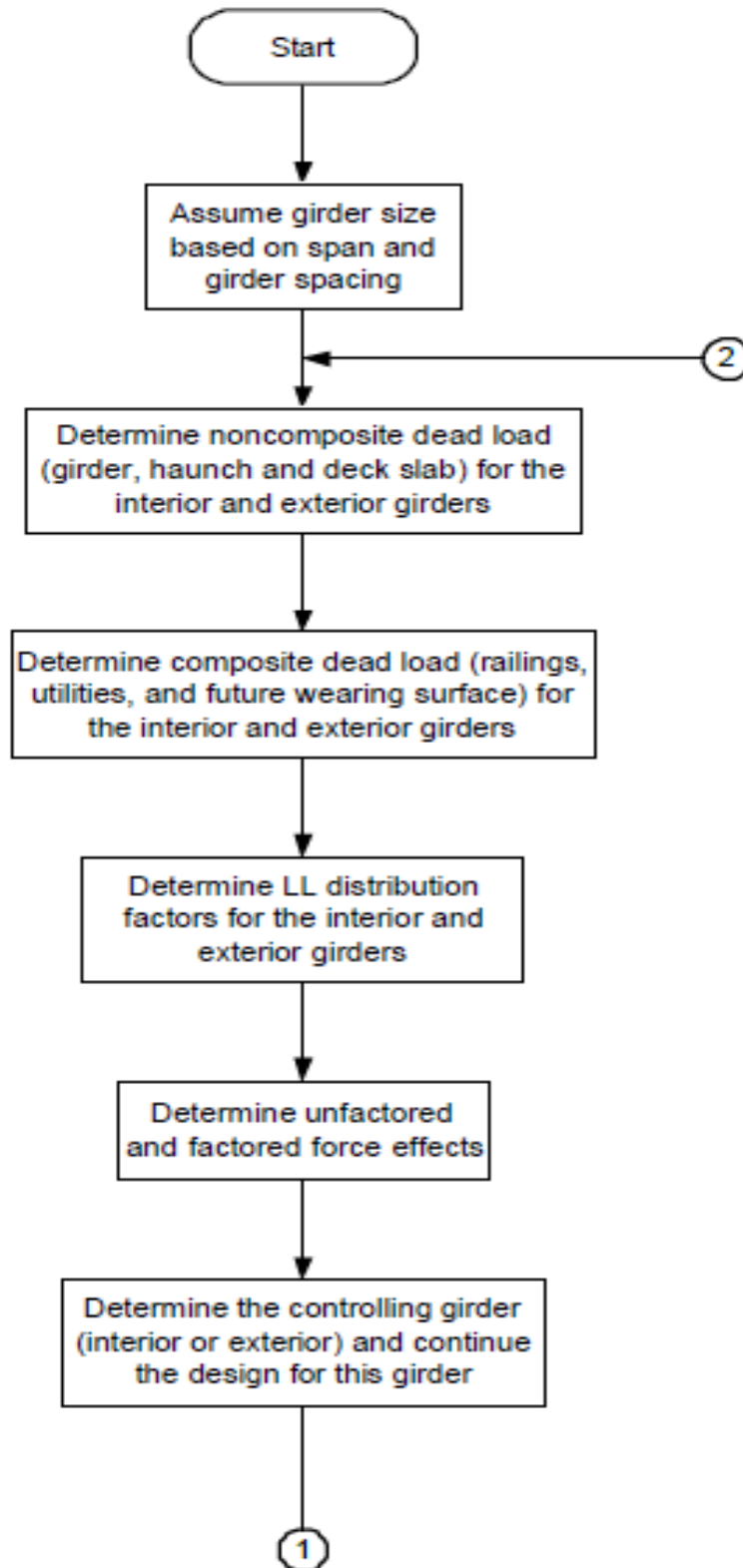


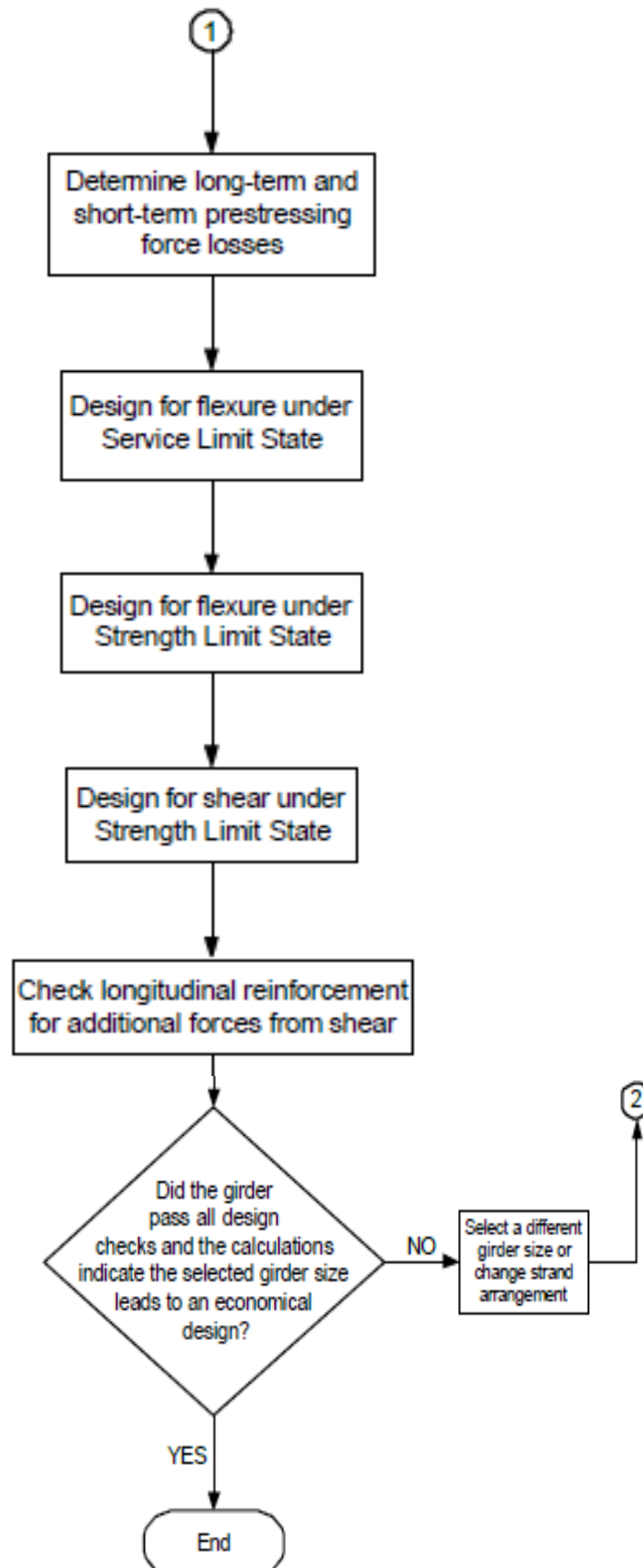
3.2 Deck Slab Design



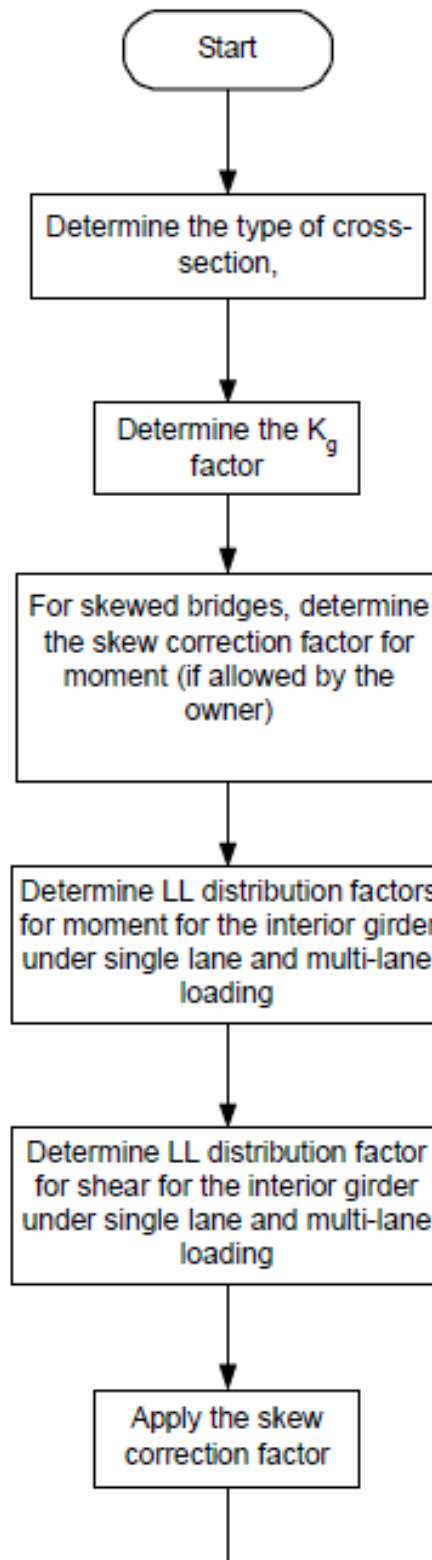


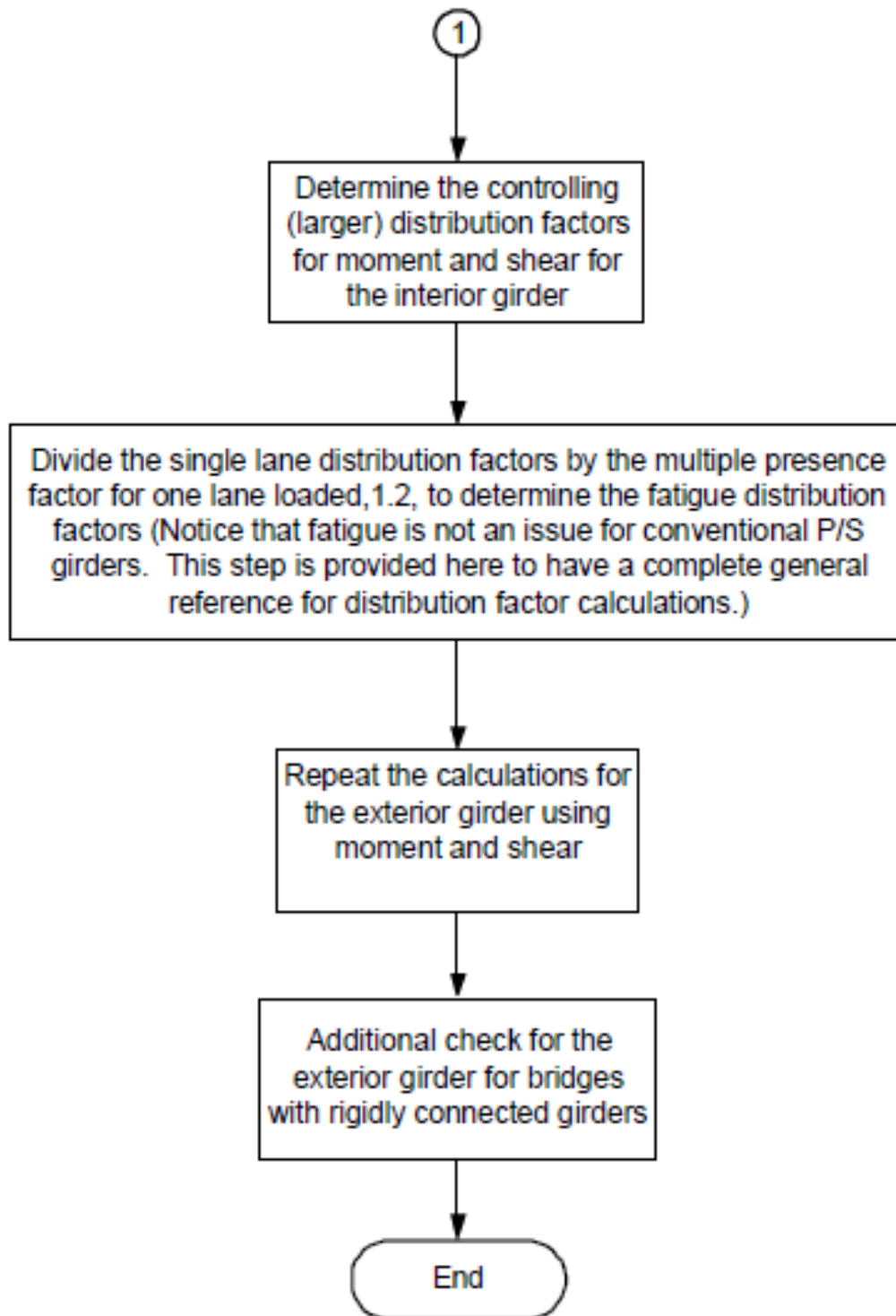
3.3 General Superstructure Design



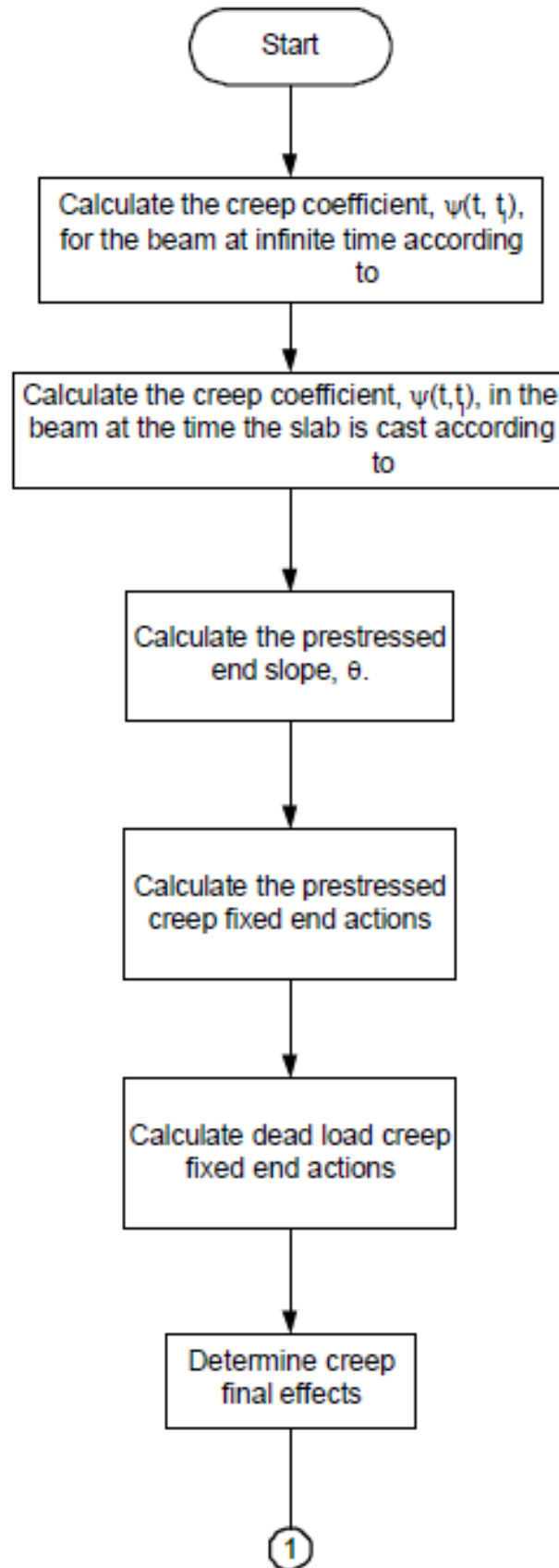


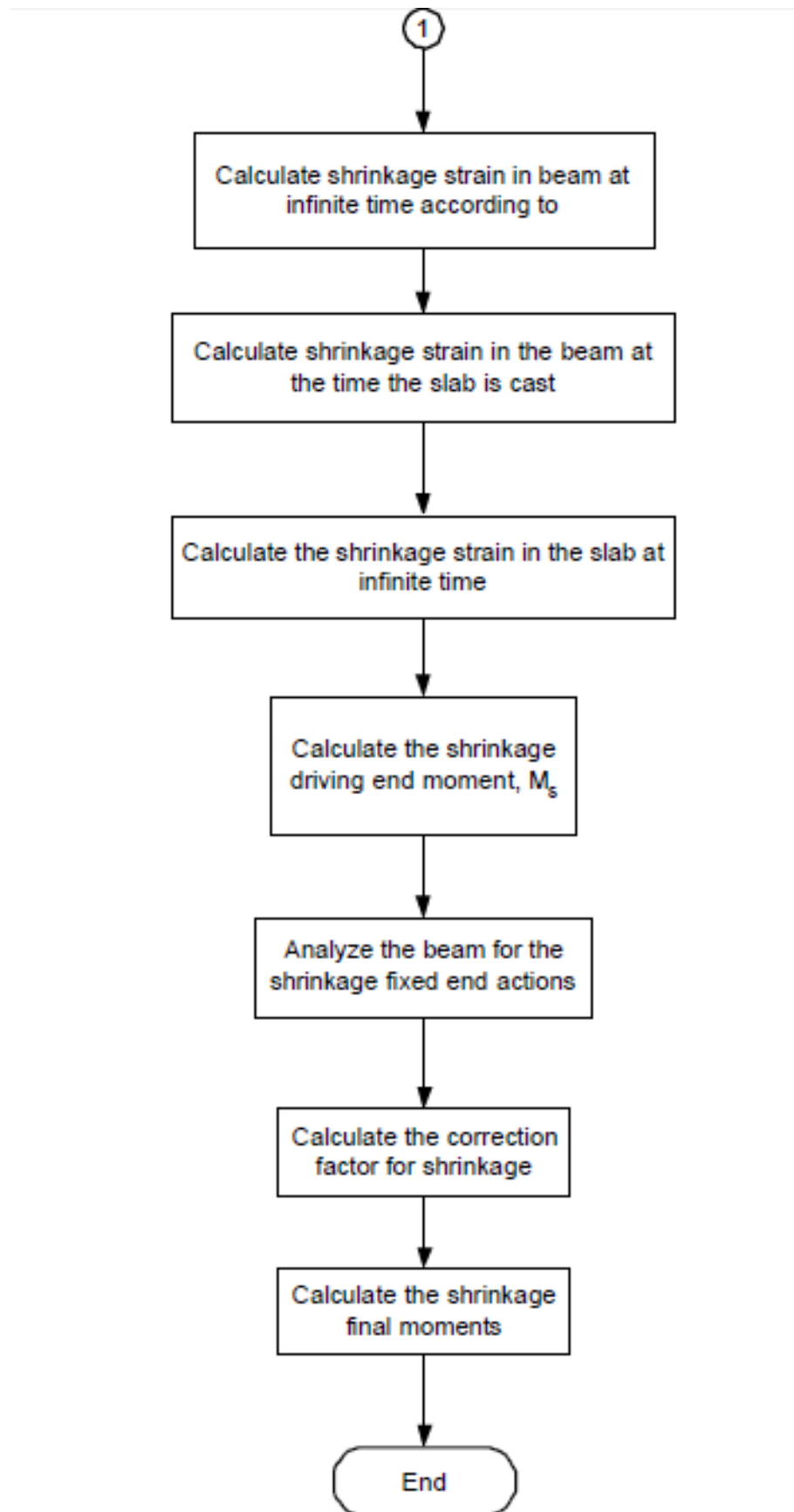
3.4 Live Load Distribution Factor Calculations



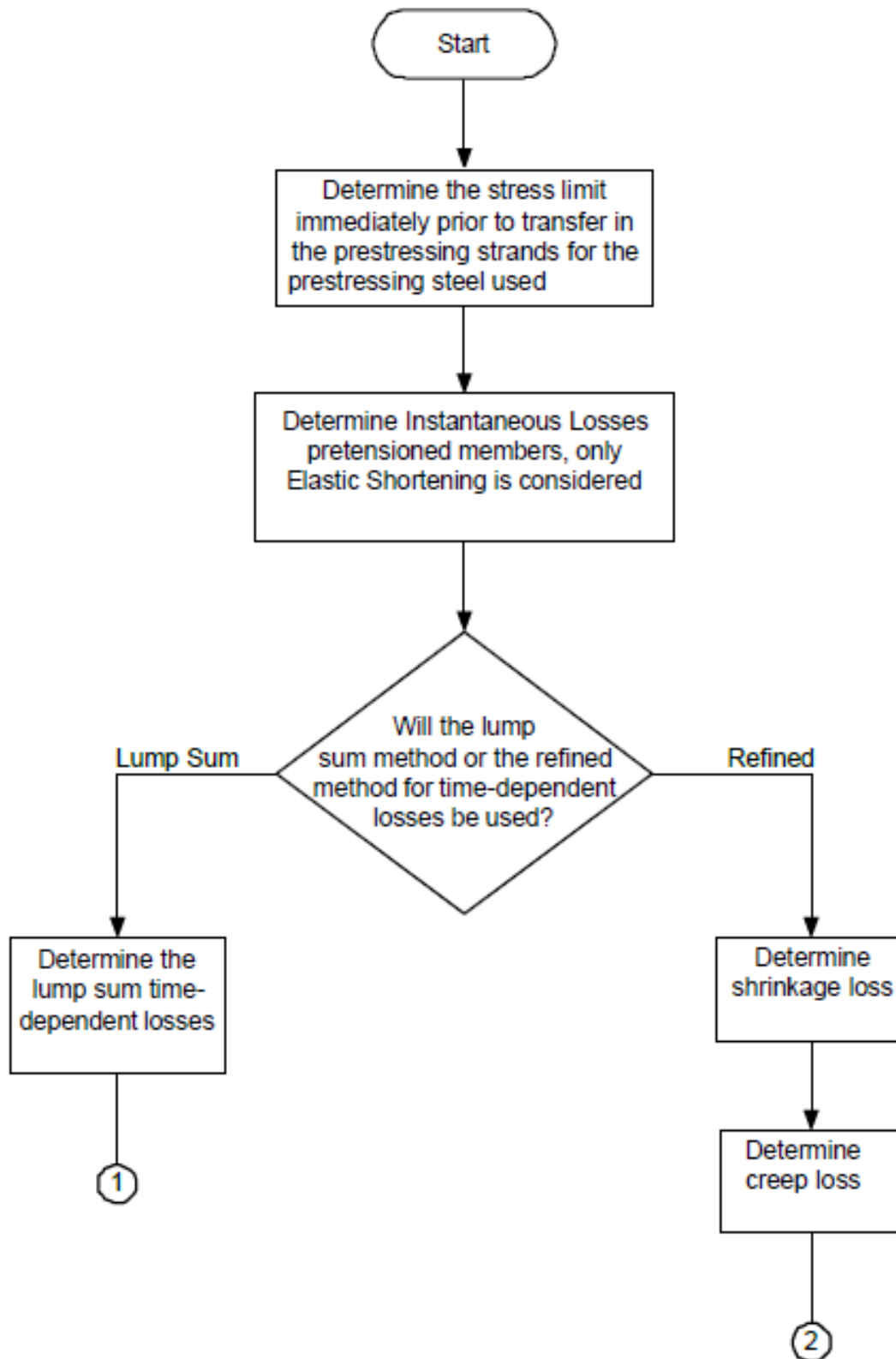


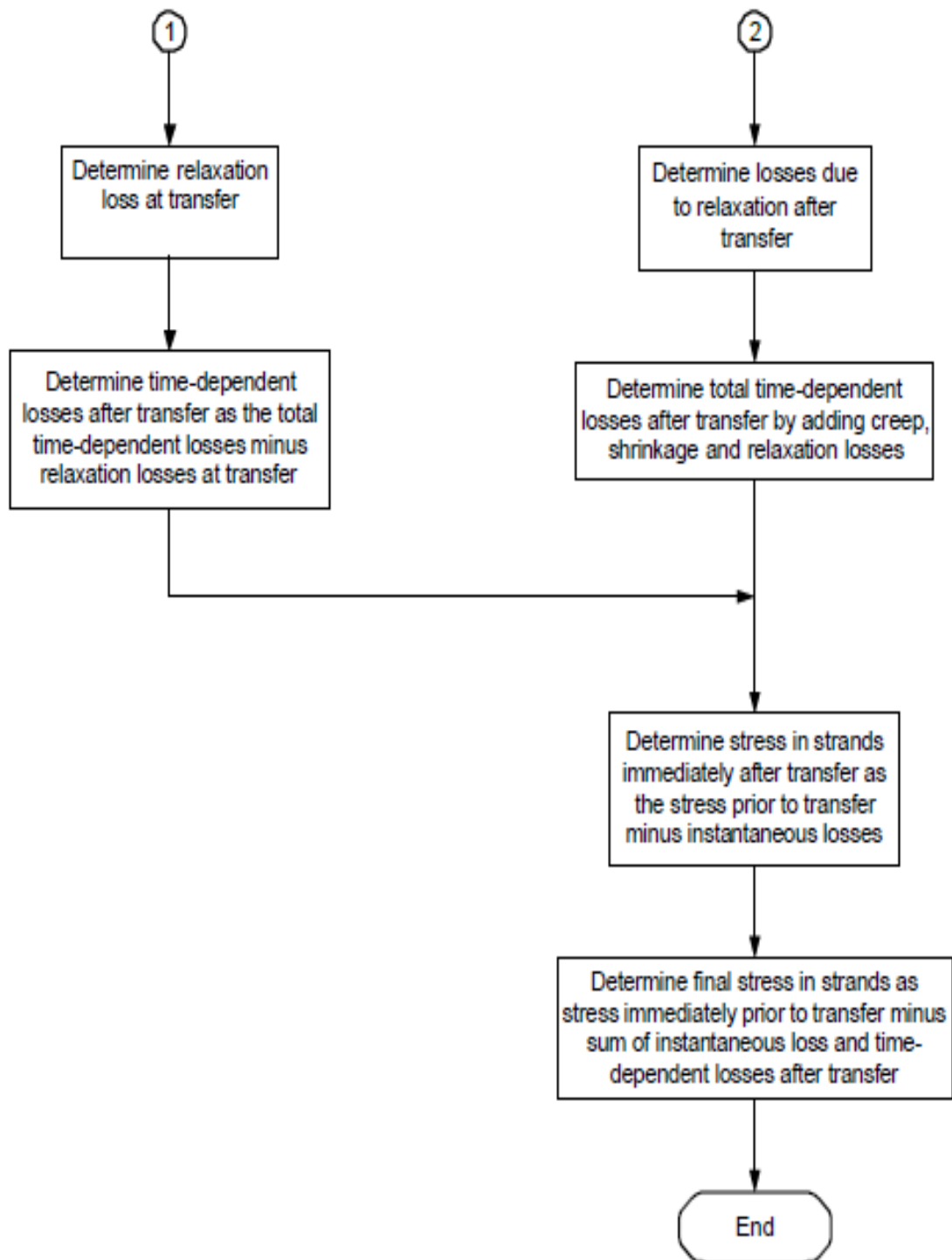
3.5 Creep and Shrinkage Calculations





3.6 Prestressing Losses Calculations





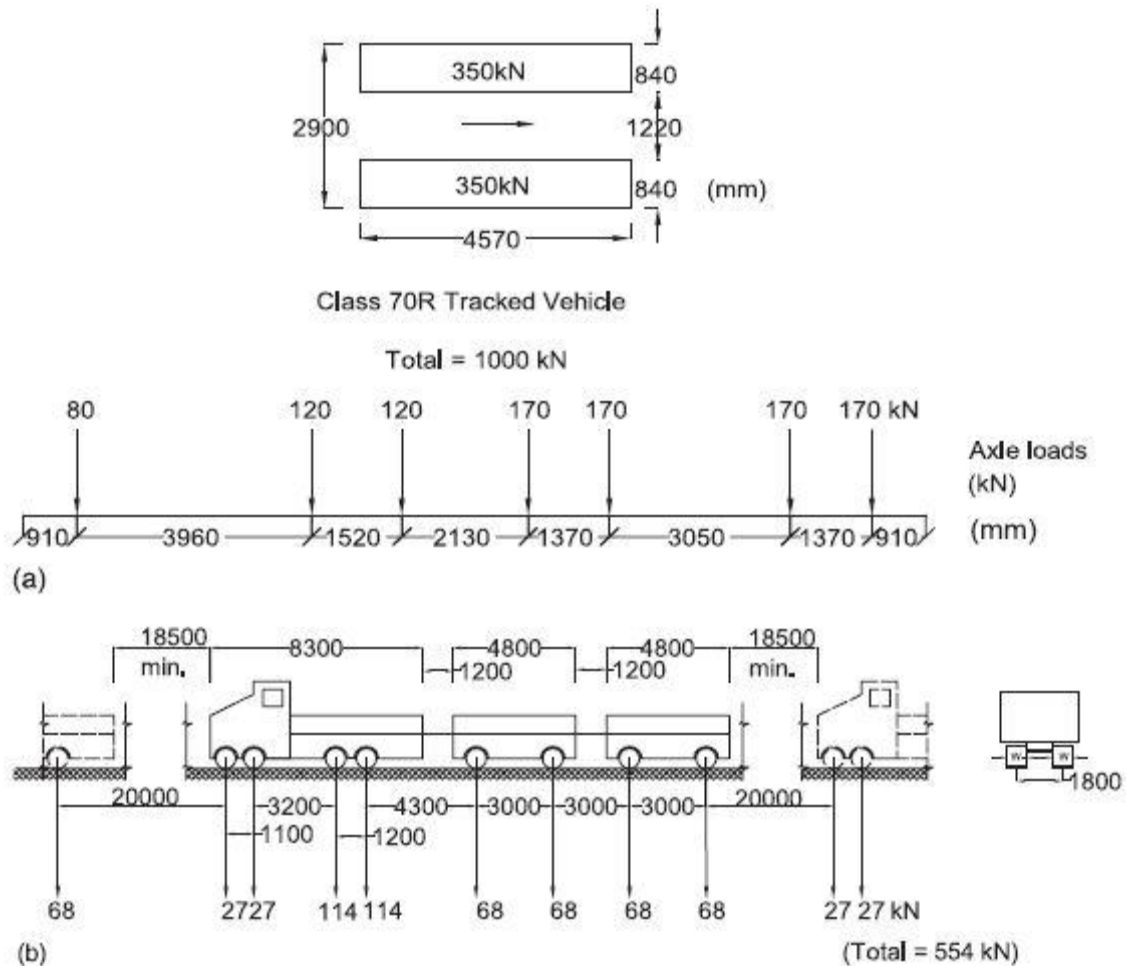


Fig. 14. Details of Class A Vehicle

4. DESIGN OF BRIDGE SUPERSTRUCTURE

- 4.1 Live load distribution factors
- 4.2 Dead load calculations
- 4.3 Unfactored and factored load effects
- 4.4 Loss of prestress
- 4.5 Stress in prestressing strands
- 4.6 Design for flexure
- 4.7 Design For Shear

5. FORMULATION

A. Loading on Box Girder Bridge

The various type of loads, forces and stresses to be considered in the analysis and design of the various components of the bridge are given in IRC6:2000 (Section II). But the common forces are considered to design the model are as follows:

Dead Load (DL):

The dead load carried by the girder or the member consists of its own weight, self-weight of the deck slab, weight of the haunch, barrier, the asphalt wearing surface and the portions of the weight of the superstructure and any fixed loads supported by the member. The dead load can be estimated fairly accurately during design and can be controlled during construction and service.

Superimposed Dead Load (SIDL):

The weight of superimposed dead load includes footpaths, earth-fills, wearing course, stay-in - place forms, ballast, water-proofing, signs, architectural ornamentation, pipes, conduits, cables and any other immovable appurtenances installed on the structure.

Live Load (LL):

Live loads are those caused by vehicles which pass over the bridge and are transient in nature. These loads cannot be estimated precisely, and the

designer has very little control over them once the bridge is opened to traffic. However, hypothetical loadings which are reasonably realistic need to be evolved and specified to serve as design criteria. There are four types of standard loadings for which road bridges are designed.

- i. IRC Class 70R loading
- ii. IRC Class AA loading

iii. IRC Class A loading

iv. IRC Class B loading

The model is design by considering IRC Class A loading, which is normally adopted on all roads on which permanent bridges and culverts are constructed.

Total load is 554,

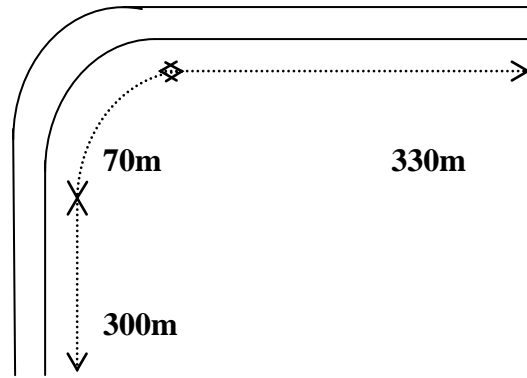


Fig. 15. Bridge Orientation

Other information regarding Live load combination as per IRC:6 2000 Clause No.207.1 Note No.4

The design live load shall consist of standard wheeled or tracked vehicles or trains of vehicles as illustrated.

B. Thickness of Web

The thickness of the web shall not be less than $d/36$ plus twice the clear cover to the reinforcement plus diameter of the duct hole where 'd' is the overall depth of the box girder measured from the top of the deck slab to the bottom of the soffit or 200 mm plus the diameter of duct holes, whichever is greater.

C. Thickness of Bottom Flange

The thickness of the bottom flange of box girder shall be not less than $1/20$ th of the clear web spacing at the junction with bottom flange or 200 mm whichever is more.

D. Thickness of Top Flange

The minimum thickness of the deck slab including that at cantilever tips be 200 mm. For top and bottom flange having prestressing cables, the

thickness of such flange shall not be less than 150 mm plus diameter of duct hole.

E. Losses in Prestress

While assessing the stresses in concrete and steel during tensioning operations and later in service, due regard shall be paid to all losses and variations in stress resulting from creep of concrete, shrinkage of concrete, relaxation of steel, the shortening (elastic deformation) of concrete at transfer, and friction and slip of anchorage.

In computing the losses in prestress when untensioned reinforcement is present, the effect of the tensile stresses developed by the untensioned reinforcement due to shrinkage and creep shall be considered.

F. Calculation of Ultimate Strength

Ultimate moment resistance of sections, under these two alternative conditions of failure shall be calculated by the following formulae and the smaller of the two values shall be taken as the ultimate moment of resistance for design:

- i. Failure by yield of steel (under-reinforced section)

$$M_{ult} = 0.9dbAsF_p$$

Where,

As = the area of high tensile steel

F_p = the ultimate tensile strength for steel without definite yield point or yield stress or stress at 4 per cent elongation whichever is higher for steel with an definite yield point.

db = the depth of the beam from the maximum compression edge to the centre of gravity of the steel tendons.

ii. Failure by crushing concrete

$$M_{ult} = 0.176 bdb^2 f_{ck}$$

Where,

b = the width of rectangular section or web of beam

f_{ck} = characteristics strength of concrete.

G. Calculation of Section un-cracked in flexure

$$\sigma_{co} = 0.67bd\sqrt{f_t + 0.8f_{cp}f_t}$$

Equation...(1)

Where,

f_t = maximum principle tensile stress given by

$$f_t = 0.24\sqrt{f_{ck}}$$

6.1 Bridge substructure geometry

Intermediate pier: Multi-column bent (13 – columns spaced at 35m Spread footings founded on sandy soil

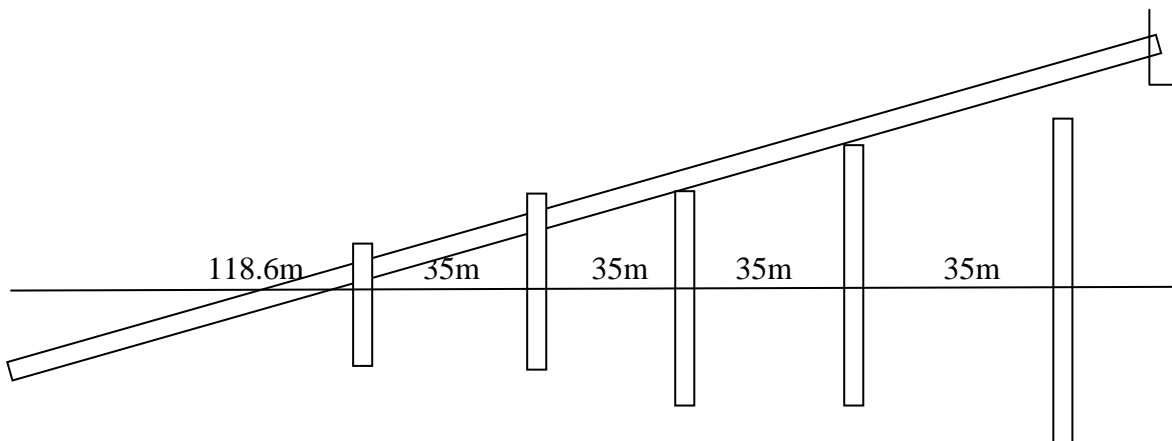


Fig. 16. Intermediate pier geometry

End abutments: supported on bedrock. U wing walls b are cantilevered from the fill face of the abutment.

b = width in the case of rectangular member and width of the rib in the case of T, I and L beams

d = overall depth of the member

f_{cp} = compressive stress at centroidal axis due to prestress taken as positive.

6. PSC BOX GIRDER BRIDGE DESIGN EXAMPLE

A two cell concrete box girder bridge with a 700 m span and is loaded with 2 traffic lanes.

The bridge has 13 columns with different heights supporting the deck at midspan. There is a prestressed tendons assigned to the deck. The bridge abutments are skewed 15 degrees at the 2 ends of the bridge deck.

Orientation of the bridge

300 m Span straight N00°00'E

70 m Span curved with radius 51 and N78°00'E

330m Span straight N78°00'E

Span= 700m

Width=10.9728m

Top Slab Thickness= 0.3048m

Bototm Slab Thickness= 0.2032m

6.2 Girder geometry and section properties

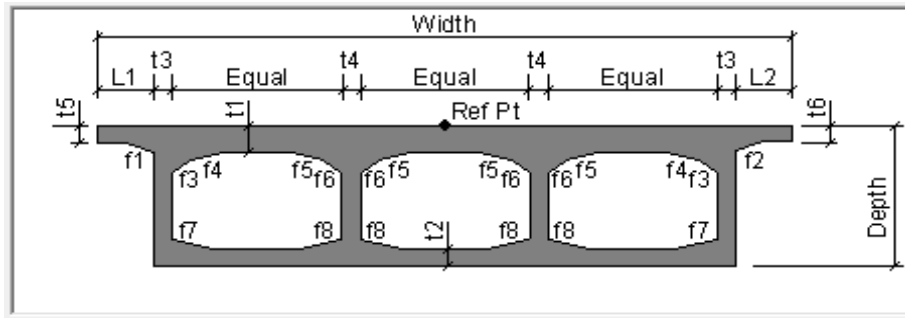


Fig. 17. Typical girder section

6.3 Slab & Girder Thickness

No. of interior girder = 1

Top slab thickness (t_1) = 0.3048m

Bottom slab thickness (t_2) = 0.2032m

Exterior Girder thickness (t_3) = 0.3048m

Interior Girder thickness (t_3) = 0.3048m

6.4 Fillet Horizontal Dimension Data

Horizontal Dimension (f_1) = 0.4572m

Horizontal Dimension (f_2) = 0.4572m

Horizontal Dimension (f_3) = 0.4572m

Horizontal Dimension (f_4) = 0.4572m

Horizontal Dimension (f_5) = 0.4572m

Horizontal Dimension (f_6) = 0.4572m

Horizontal Dimension (f_7) = 0.4572m

Horizontal Dimension (f_8) = 0.4572m

6.5 Fillet Vertical Dimension Data

Vertical Dimension (f_1) = 0.1524m

Vertical Dimension (f_2) = 0.1524m

Vertical Dimension (f_3) = 0.1524m

Vertical Dimension (f_4) = 0.1524m

Vertical Dimension (f_5) = 0.1524m

Vertical Dimension (f_6) = 0.1524m

Vertical Dimension (f_7) = 0.1524m

Vertical Dimension (f_8) = 0.1524m

6.6 Left Overhang Data

Left Overhang (L_1) = 0.9144m

Left Overhang Outer Thickness (t_5) = 0.2032m

6.7 Right Overhang Data

Right Overhang (L_2) = 0.9144m

Right Overhang Outer Thickness (t_6) = 0.2032m

6.8 Design Data

Top slab cut line distance (from top of section) = 0.6096m

Bottom slab cut line distance (from bottom of section) = 0.35567m

Basic beam section properties

Beam length, $L = 110 \text{ ft.} - 6 \text{ in.}$

6.9 Tendon Data

The tendon profile is considered as parabolic in nature.

As per IRC:18-2000

$f_{ck} = 50 \text{ Mpa}$, $f_{ci} = 0.8f_{ck} = 40 \text{ Mpa}$, $f_{ct} = 0.5$, $f_{ci} = 20 \text{ Mpa}$, $f_{cw} = 0.33f_{ck} = 16.5 \text{ Mpa}$, $f_t = 1/10f_{ct} = 2.0 \text{ Mpa}$, $f_{tw} = 0$

As per IS:1343-1980

$E_c = 5700f_{ck}^{1/2} = 40.30 \text{ kN/m}^2$, $f_p = 1862 \text{ Mpa}$, $n = 0.85$, $E = 2 \times 10^5 \text{ Mpa}$

Torsional Constant = 559708.2

Moment of Inertia = 279854.08 mm^4

Shear Area = 1687.77 mm^2

Tendon area = 645.16 mm^2

Maximum discretization length = 1.524m

6.10 Friction & Anchorage Losses

Curvature coefficient = 0.15

Wobble coefficient = $3.281 \times 10^{-3} \text{ 1/m}$

Anchorage set slip = $6.350 \times 10^{-3} \text{ m}$

6.11 Other Loss Parameters

Elastic shortening stress = 20684274 N/m^2

Creep stress = 34473789 N/m^2

Shrinkage stress = 48263305 N/m^2

Steel relaxation stress = 34473789 N/m^2

The Strand Pattern:

The strand pattern and number of strands was initially determined based on past experience and subsequently refined using a computer design program. This design was refined using trial and error until a pattern produced stresses, at transfer and under service loads, that fell within the permissible stress limits and produced load resistances greater than the applied loads under the strength limit states. For debonded strands, the number of partially debonded strands should not exceed 25 percent of the total number of strands. Also, the number of debonded strands in any horizontal row shall not exceed 40 percent of the strands in that row. The selected pattern has 27.2 percent of the total strands debonded. This is slightly higher than the 25 percent stated in the specifications, but is acceptable since the specifications require that this limit “should” be satisfied. Using the word “should” instead of “shall” signifies that the specifications allow some deviation from the limit of 25 percent. Typically, the most economical strand arrangement calls for the strands to be located as close as possible to the bottom of the girders. However, in some cases, it may not be possible to satisfy all specification requirements while keeping the girder size to a

minimum and keeping the strands near the bottom of the beam. This is more pronounced when debonded strands are used due to the limitation on the percentage of debonded strands. In such cases, the designer may consider the following two solutions:

- Increase the size of the girder to reduce the range of stress, i.e., the difference between the stress at transfer and the stress at final stage.
- Increase the number of strands and shift the center of gravity of the strands upward. Either solution results in some loss of economy. The designer should consider specific site conditions (e.g., cost of the deeper girder, cost of the additional strands, the available under-clearance and cost of raising the approach roadway to accommodate deeper girders) when determining which solution to adopt.

7. VALIDATION OF RESULTS

The bending moment, shear force and deflection result obtained by SAP 2000. The bending moment and shear force are calculated by considering different loading condition such as dead load, live load and superimposed load. Same as deflection calculated.

7.1 SAP Design Module:

a) Bridge Geometry

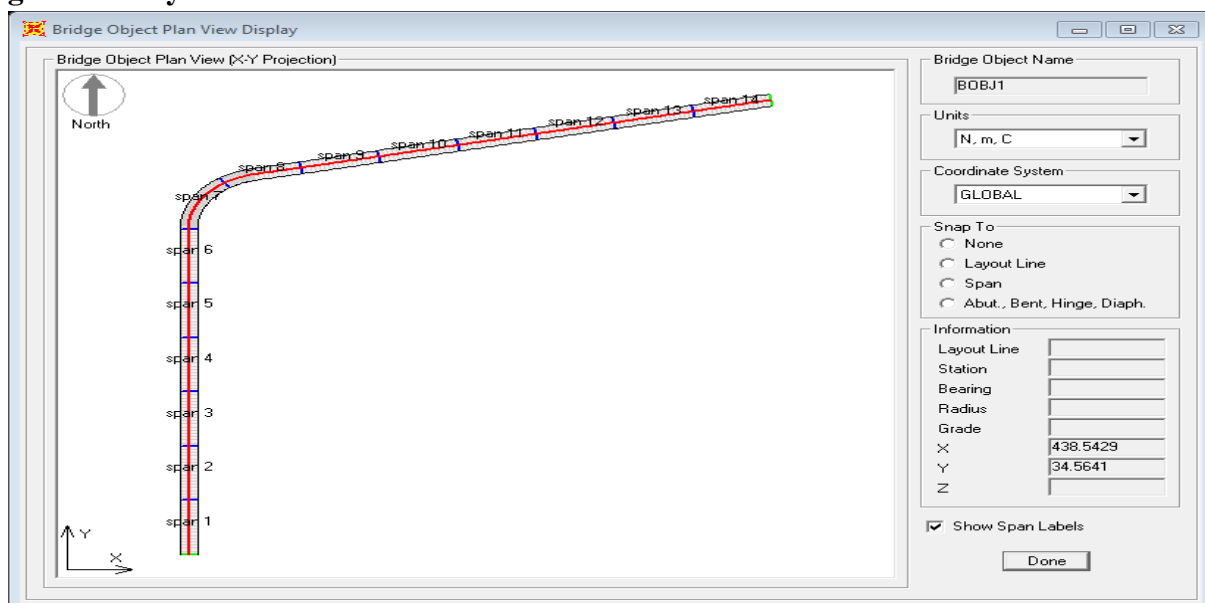


Fig. 18. Bridge In Plan

3D View

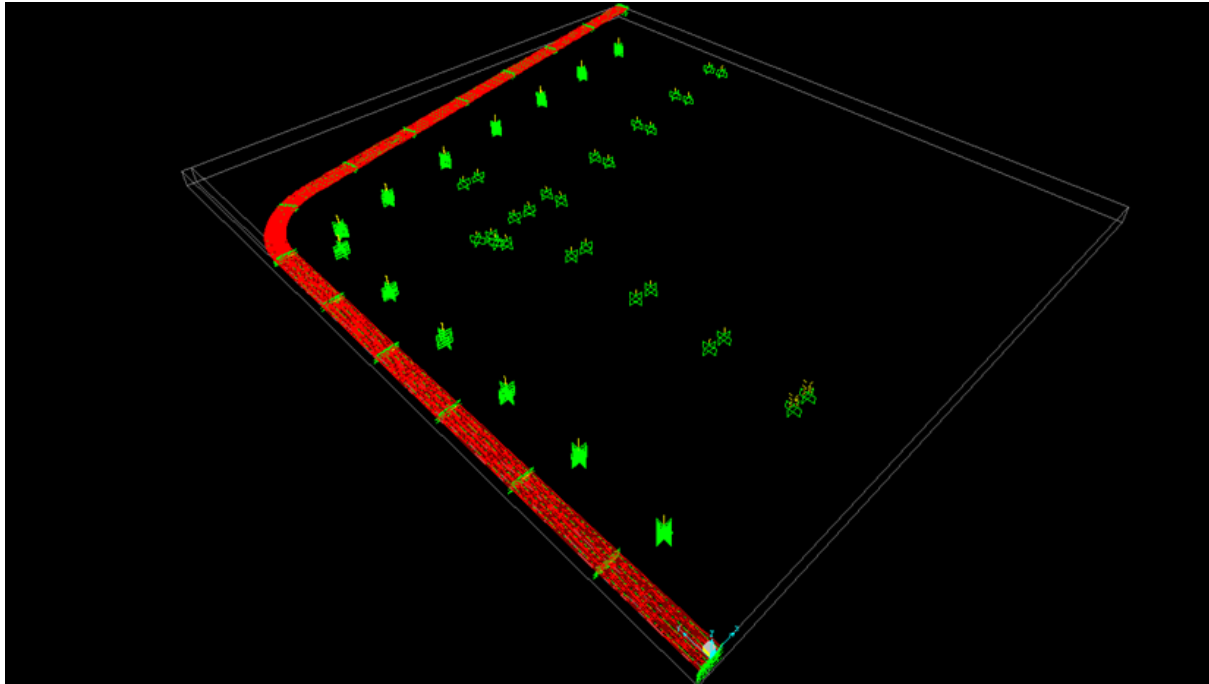


Fig. 19. 3D View Of Bridge

XY Plane View

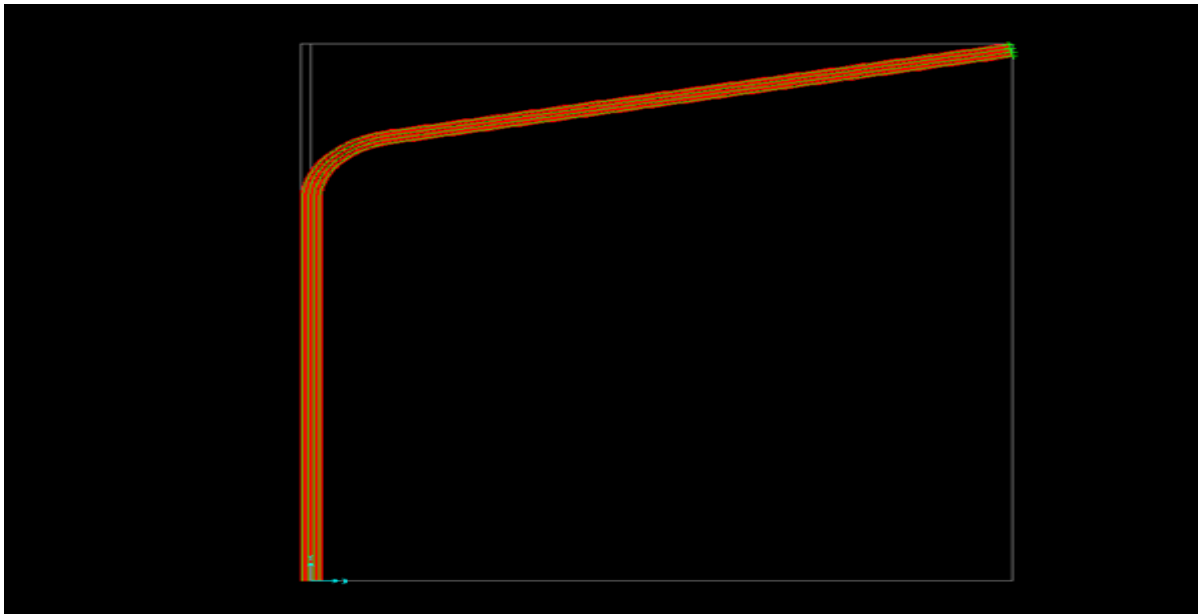


Fig.20. XY plane view in SAP

7.2 Bridge Object Response Values

Table I Bridge Object Response Values of Force, Shear, Torsion, Moments

Distance	Axial Force	Shear Vertical	Shear Horizontal	Torsion	Moment @ Vertical axis	Moment @ Hzl axis
L	P	V2	V3	T	M2	M3
m	KN	KN	KN	N-m	N-m	N-m
0	-9169	-65863	-13788	-8956355846	-2831531405	-8230652
50	-9169	-65863	-13788	-8956354331	-2139496314	3049961759
50	-9169	-65863	-13788	-8956354510	-2139499272	3049782548
100	-9169	-65863	-13788	-8956358109	-1421746756	5641795923
100	-9169	-65863	-13788	-8956355449	-1479774408	5641616496
150	-9169	-65863	-13788	-8956357368	-724257238	7767693457
150	-9169	-65863	-13788	-8956352825	-801696255	7767495293
200	-9169	-65863	-13788	-8956352823	-42211679	9427629643
200	-9169	-65863	-13788	-8956357733	-119694485	9427546390
250	-9169	-65863	-13788	-8956355792	635833829	10620000000
250	-9169	-65863	-13788	-8956357487	577799804	10620000000
300	-9169	-65863	-13788	-8956249390	1345535954	11350000000
300	-9169	-65863	-13788	-8821674817	1165632411	11440000000
350	-9169	-65863	-13788	4550974072	1715661822	13970000000
350	-9169	-65863	-13788	4690857459	1767959831	13920000000
400	-9169	-65863	-13788	9496071044	1493032245	11020000000
400	-9169	-65863	-13788	9496077330	1565736129	11020000000
450	-9169	-65863	-13788	9496075091	1252561087	10350000000
450	-9169	-65863	-13788	9496073216	1314076788	10350000000
500	-9169	-65863	-13788	9496075236	1002194091	9211954727
500	-9169	-65863	-13788	9496072706	1084329951	9212029247
550	-9169	-65863	-13788	9496072673	768233137	7610313247
550	-9169	-65863	-13788	9496075727	850293699	7610501473
600	-9169	-65863	-13788	9496073633	538345522	5542796789
600	-9169	-65863	-13788	9496076346	599837482	5542967682
650	-9169	-65863	-13788	9496078478	286443029	3009335810
650	-9169	-65863	-13788	9496073226	358774115	3009499584
697	-9169	-65863	-13788	9496068271	193271103	198793779
700	-9169	-65863	-13788	9496070895	107467313	9853112

7.3 Bridge Object Response Display

7.3.1 Axial force (P) of entire section and all girders

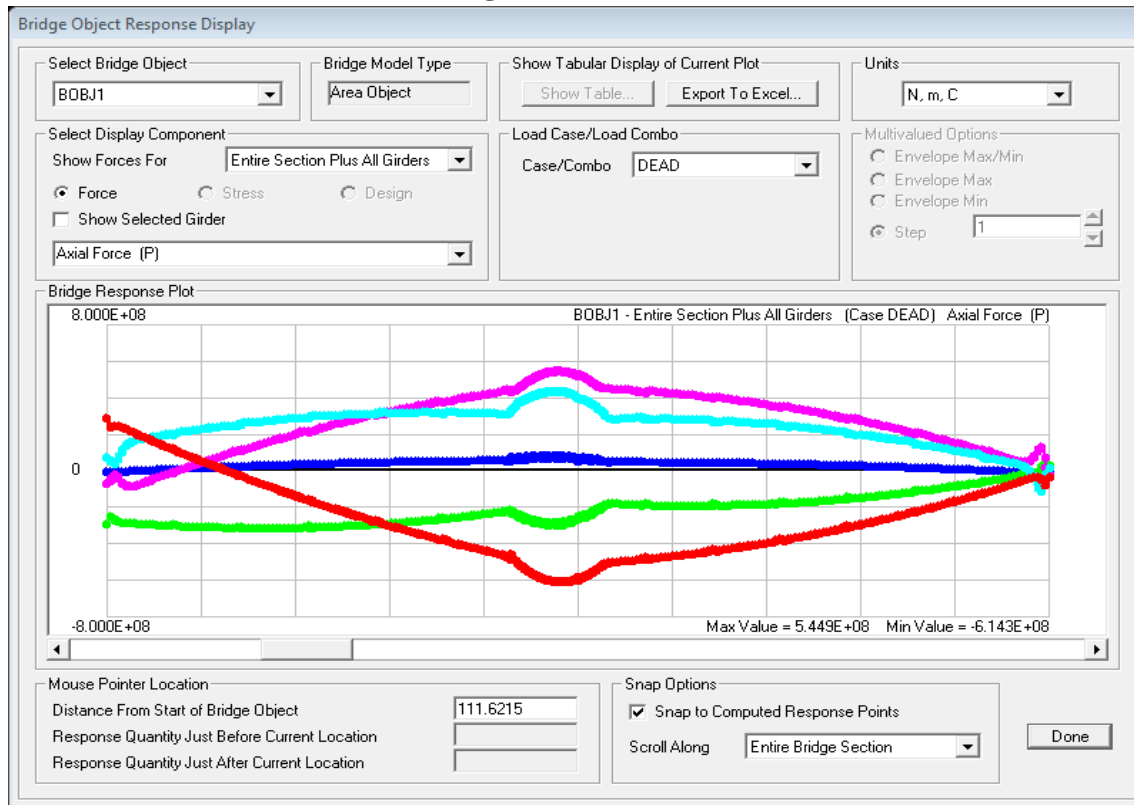


Fig. 21. Dead load

7.3.2 Vertical shear (V2) of entire section and all girders

Dead Load

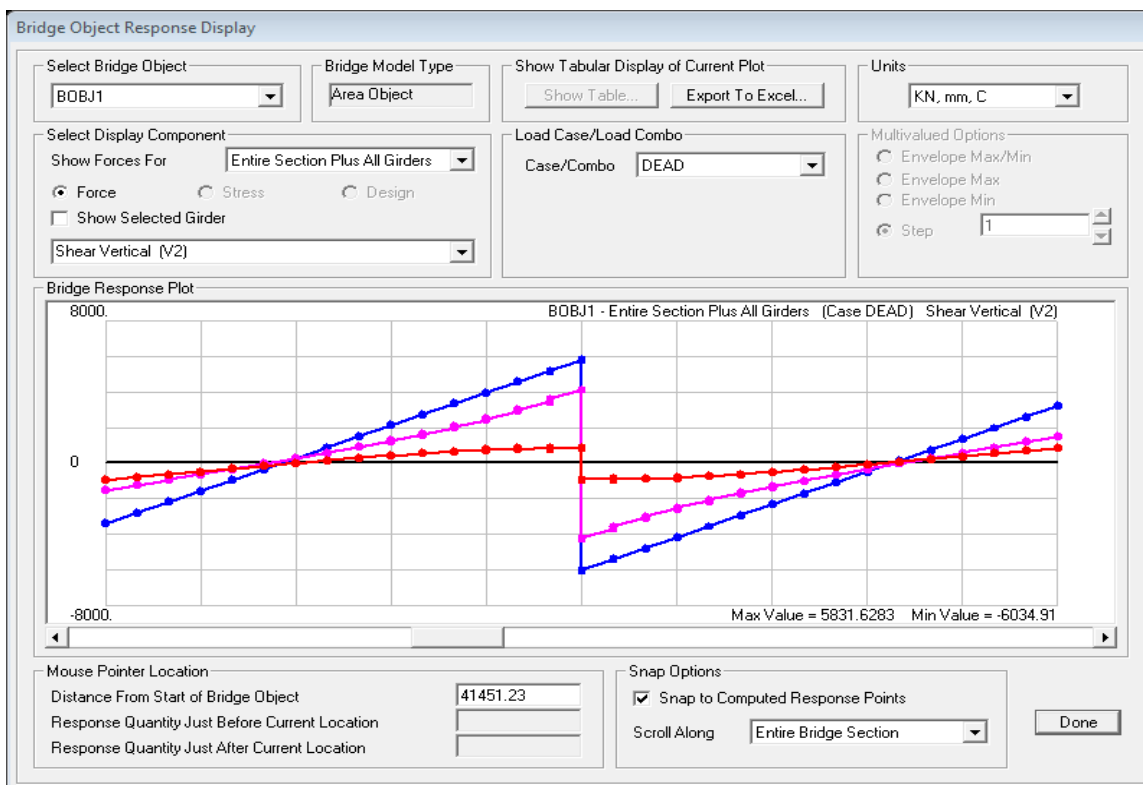


Fig. 22. Dead load

7.3.3 Shear horizontal (V3) of entire section and all girders

Dead Load

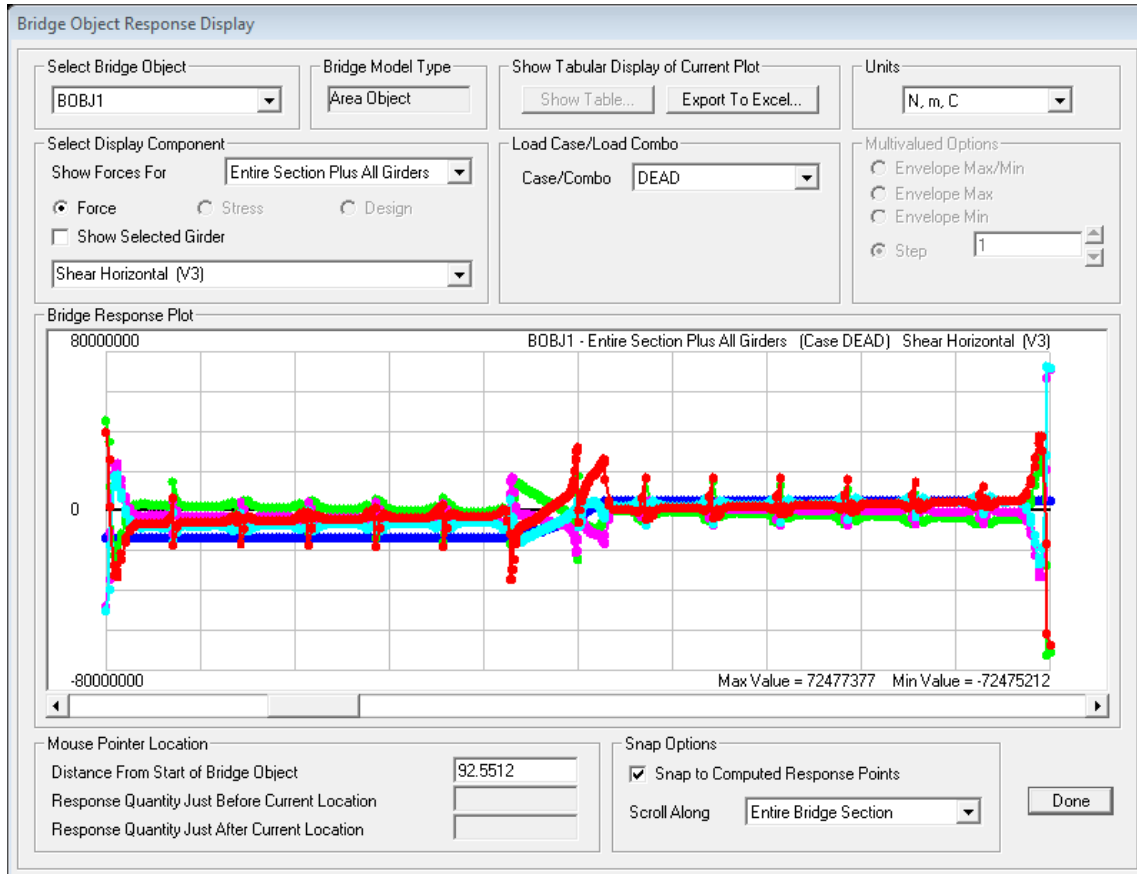


Fig.23. Dead load

7.3.4 Torsion (T) of entire section and all girders

Dead Load

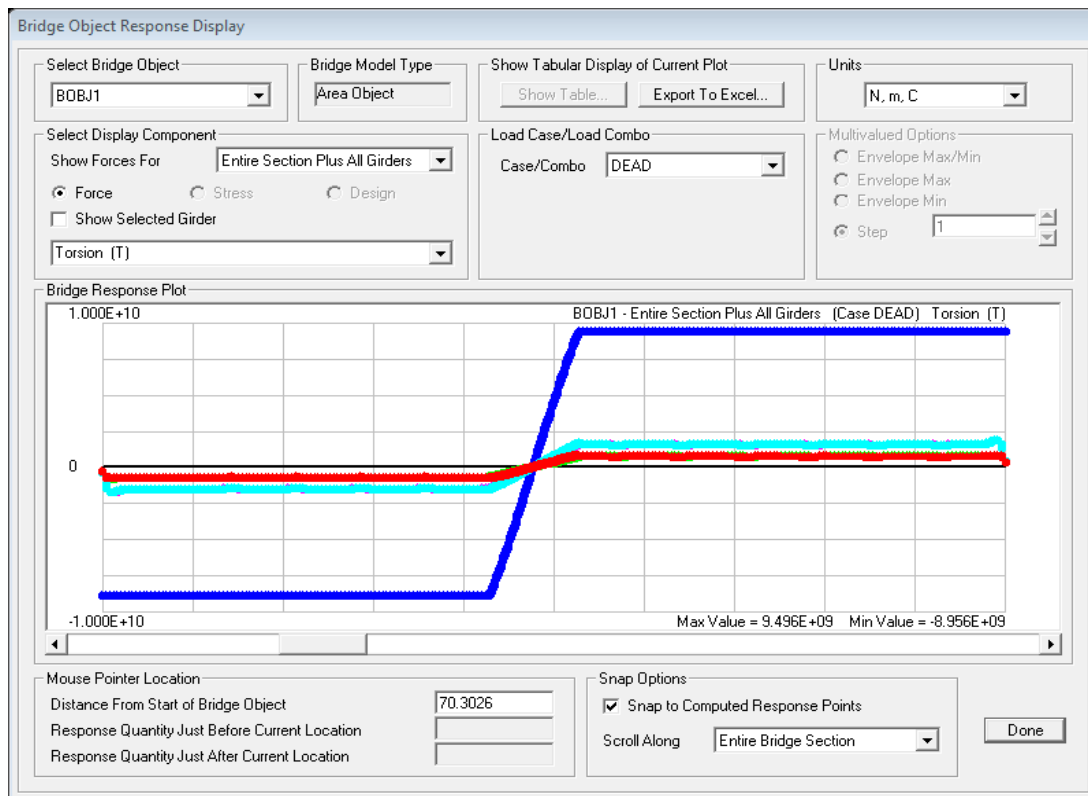


Fig.24. Dead load

7.3.5 Moment about vertical axis (M2) of entire section and all girders

Dead Load

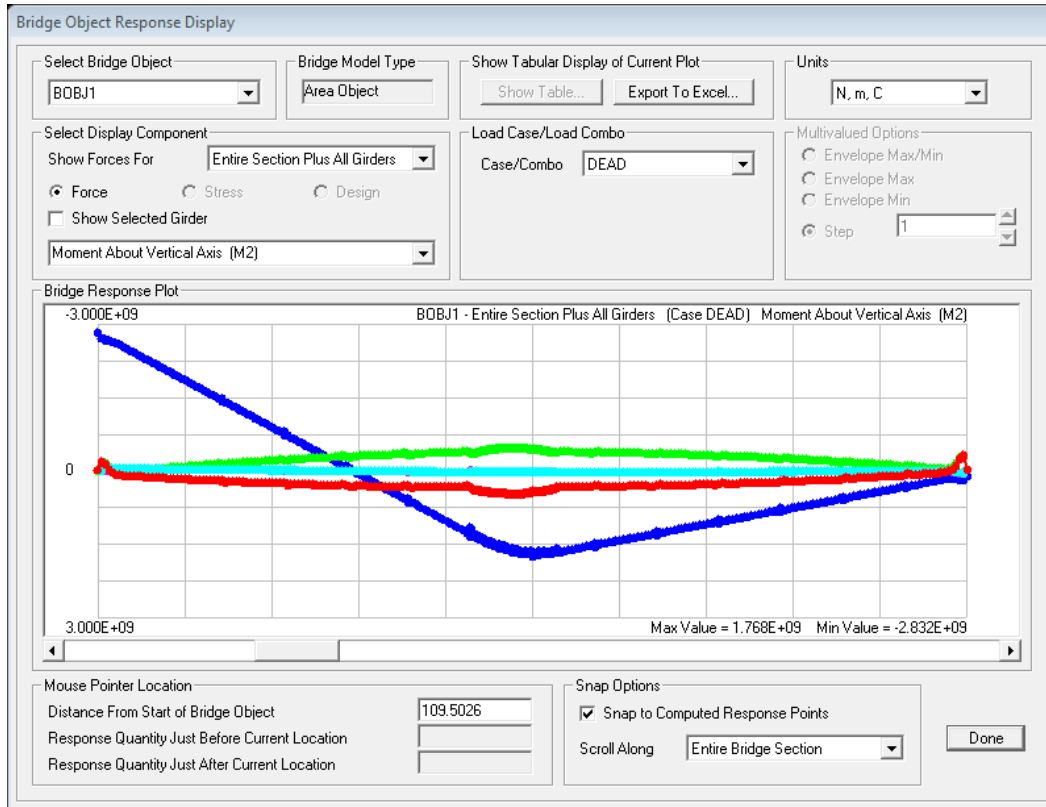


Fig.25. Dead load

7.3.6 Moment about horizontal axis (M2) of entire section and all girders

Dead Load

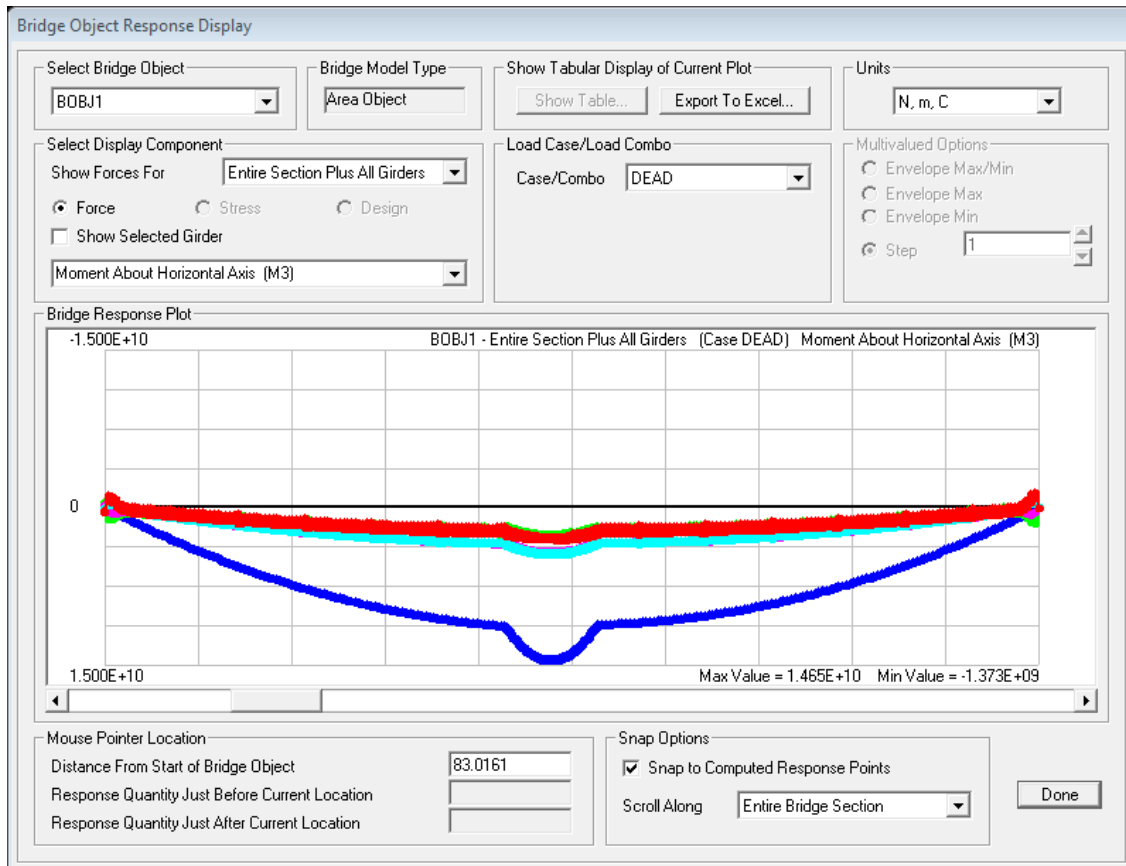


Fig.26. Dead load

7.4 Deformed Shape

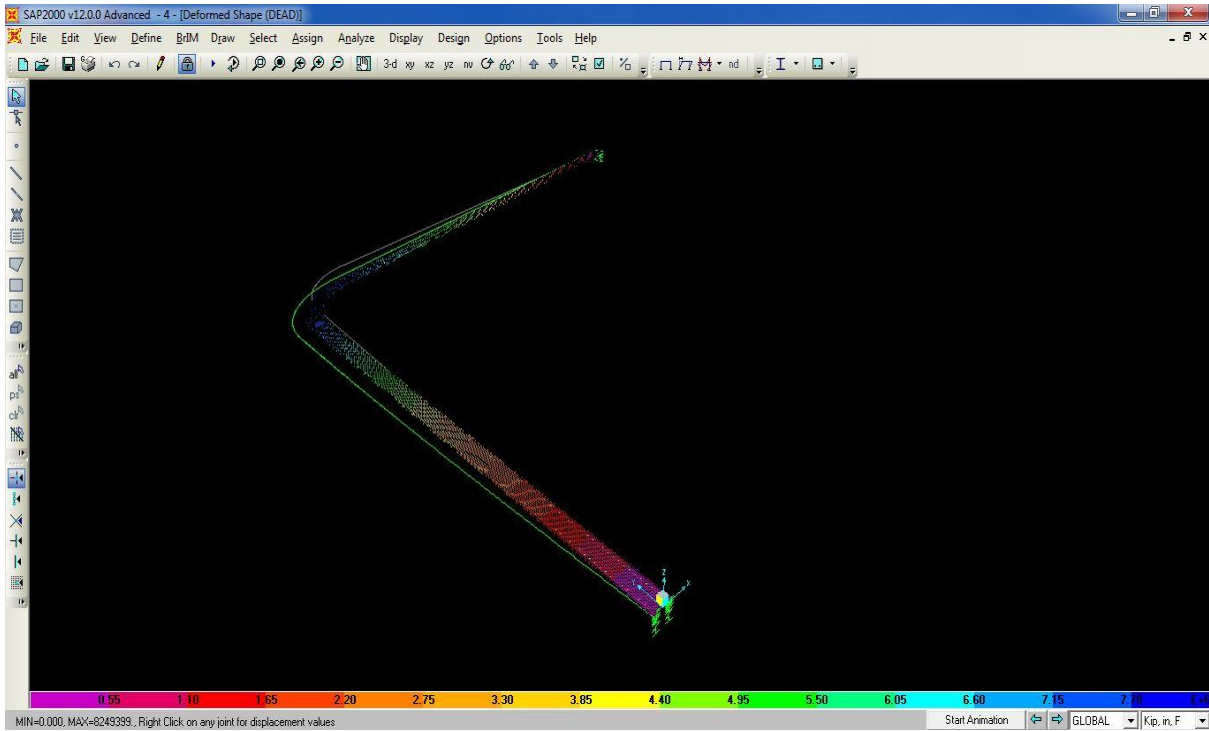


Fig.27. Influence Displacement For Moving Load

7.5 Tendon Calculated Load Data:

Table II Tendon calculated load data

Tendon	Load Pat	Load Type	Force N	Jack From	Curvature Unitless	Wobble 1/m	Loss Anchor m	Loss Short N/m2	E	Loss Creep N/m2	Loss Shrink N/m2	Loss SRelax N/m2
TEN2	DEAD	Force	444822	I-End	0.15	0.00328	0.00635	20684274	34473789	48263305	34473789	34473789
TEN3	DEAD	Force	444822	I-End	0.15	0.00328	0.00635	20684274	34473789	48263305	34473789	34473789
TEN4	DEAD	Force	444822	I-End	0.15	0.00328	0.00635	20684274	34473789	48263305	34473789	34473789
TEN5	DEAD	Force	444822	I-End	0.15	0.00328	0.00635	20684274	34473789	48263305	34473789	34473789

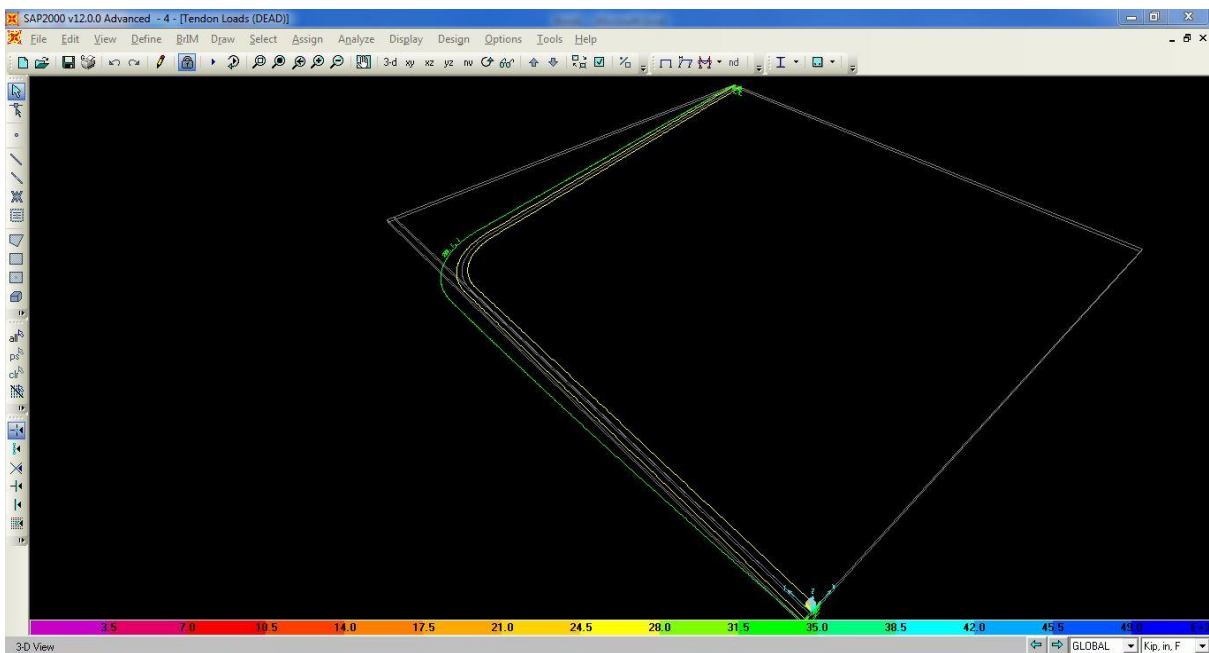


Fig.35. Tendon Load

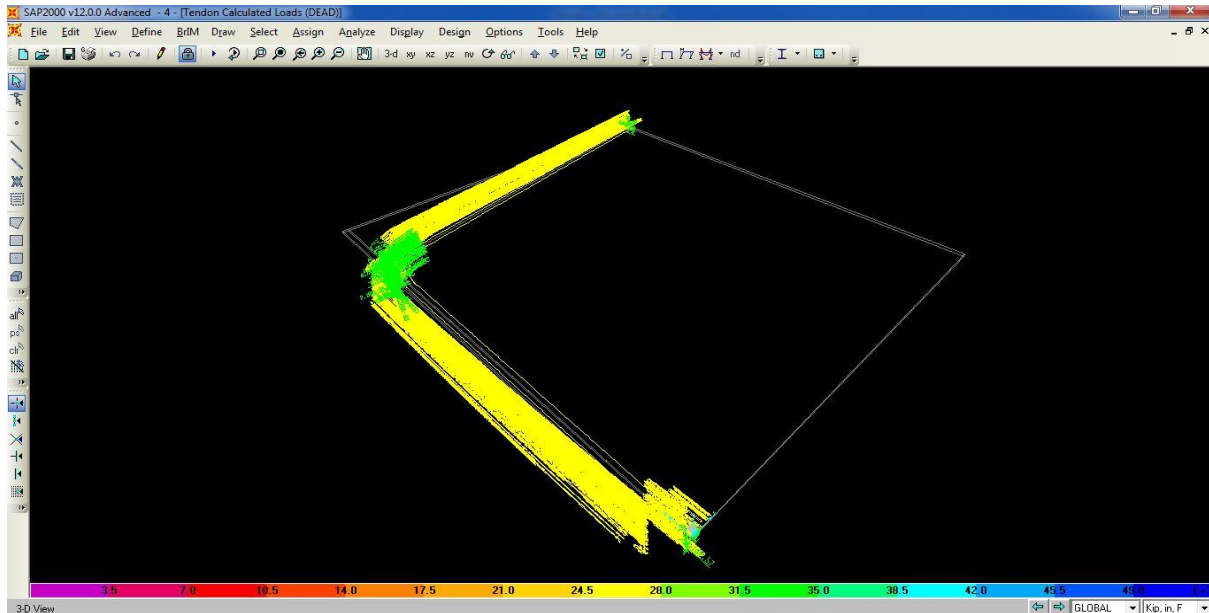


Fig.36. Tendon Calculated Load Data

7.6 Virtual Work

Dead Load

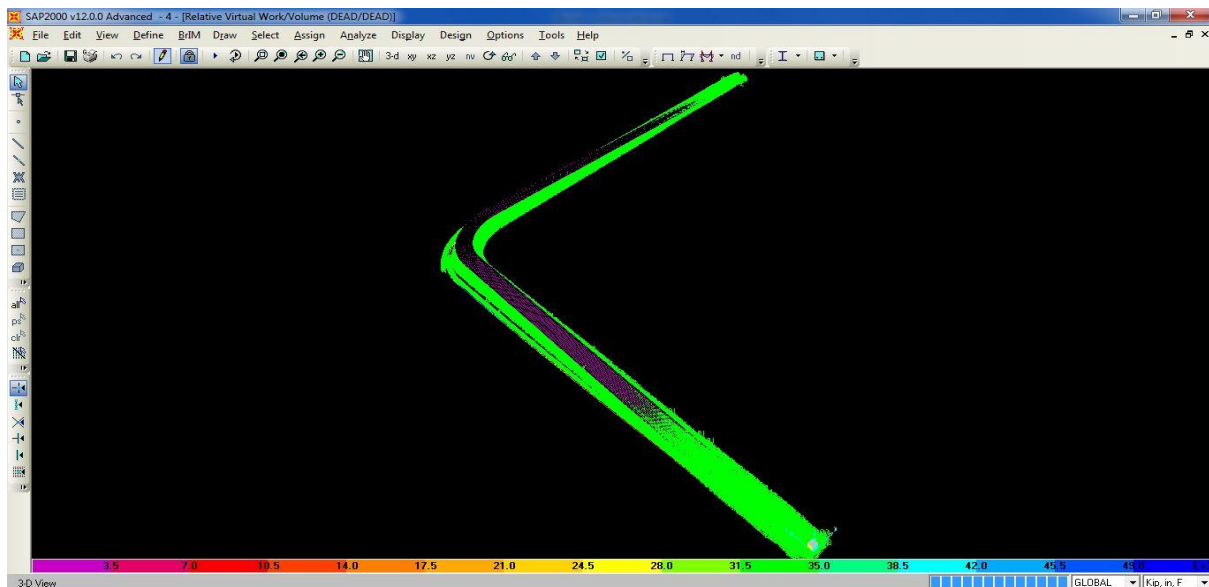


Fig.37. Dead Load

8. CONCLUSION

This paper gives basic principles for portioning of concrete box girder to help designer. Box girder shows better resistance to the torsion of superstructure. Development of time dependent and thermal strains and corresponding deflections in PSC bridge superstructure, the service life is reduced in long run. Extensive research works are required to develop smart concrete structures, replacing a percentage of conventional steel reinforcement (Fe-415/500) with superelastic alloy.

REFERENCES

1. IRC: 18 – 2000 “ DESIGN CRITERIA FOR PRESTRESSED CONCRETE ROAD BRIDGES (POST – TENSIONED CONCRETE)” THE INDIAN ROADS CONGRESS.
2. IRC: 6- 2000 “STANDARD SPECIFICATIONS AND CODE OF PRACTICE FOR ROAD BRIDGES”THE ROAD CONGRESS.

3. IS: 1343 – 1980 “ CODE OF PRACTICE FOR PRESTRESSED CONCRETE” INDIAN STANDARD.
4. Andre Picard and Bruno Massicotte, Member “SERVICEABILITY DESIGN OF PRESTRESSED CONCRETE BRIDGES” JOURNAL OF BRIDGE ENGINEERING / FEBRUARY 1999
5. ABAQUS [Computer software]. Dassault Systèmes/SIMULIA, Providence, Rhode Island.
6. Abbas, S., and Scordelis, A. C. (1993). “Nonlinear geometric, material and time-dependent analysis of segmentally erected three-dimensional cable stayed bridges.” UCB/SEMM-93/09, Univ. of California at Berkeley, Berkeley, CA.
7. American Concrete Institute (ACI). (1982). “Prediction of creep, shrinkage, and temperature effects in concrete structures.” ACI 209R-82, ACI Committee 209, Detroit, MI.
8. Ates, S. (2011). “Numerical modelling of continuous concrete box girder bridges considering construction stages.” App. Math. Model., 35(8), 3809–3820.
9. ACI 209R-92 “Prediction of creep, shrinkage and temperature effects in concrete structures” ACI Manual of Concrete practice, Part 1. Detroit: American concrete Institute; 1992.
10. Bazant, Z.P and Liu, K.L (1985) “ Random creep and shrinkage in structures: Sampling” Journal of structural engineering, ASCE, Vol.111, No.5
11. Branco, F.A (1986); Thermal effects on composite box girder bridges during construction” Proc., 2nd Int. Conf.On Short & Medium span bridges. Canadian society for civil engineering.